의학박사 학위논문

The effect of IL-23-producing human lung cancer cells on tumor growth via conversion of innate lymphoid cell 1 (ILC1) into ILC3

폐암 세포 유래 인터루킨-23에 의한 선천성 림프구 세포 1형에서 3형으로의 변환이 종양 성장에 미치는 영향 연구

2019 년 8 월

서울대학교 대학원

의학과 병리학 전공

고 재 문

Abstract

Due to the recent success of immunotherapy in non-small cell lung cancer (NSCLC) patients, there has been a growing interest in the role of immune cells in tumor microenvironment (TME). Innate lymphoid cell (ILC) is one kind of immune subsets which might contribute to the TME yet relatively unexplored. ILC has three subsets classified according to their transcription factor and cytokine expression, however, the plasticity between ILC subsets has been reported in the inflammatory bowel disease by *in vitro* experiments. Up to now, the effect of ILC subsets and their plasticity with changes in cytokines on TME has not been fully investigated. This study aimed to reveal the role of ILC plasticity and significance for potential therapeutic target in human lung TME.

ILC subsets and cytokine expression profiles were evaluated in 80 cases of NSCLC each consisting of 40 squamous cell carcinoma (SqCC) and 40 adenocarcinoma (ADC) with matched normal lung tissue, which were freshly collected in Seoul National University Hospital. Experimental conversion of ILC1 into ILC3 under co-culture with lung cancer cells was explored. The contribution of IL-23 on tumor growth and regulation of immune components in TME was investigated using *in vivo* mouse tumor model. Verification and prognostic effects of converted ILC3 and related pathways were evaluated by tissue microarray from retrospective cohort composed of 875 lung cancer patients.

As a result, IL-17RA expression on tumor cells and IL-17A expression on immune cells from TME were significantly higher in SqCC than ADC, which suggests that IL-17 has pro-tumoral effects in pulmonary SqCC. Among IL-17$^+$ cells, the percentages of ILCs were higher in SqCC than ADCs, and also ILC3s were more frequent that ILC1s in SqCC in contrast to ADC or normal lung tissue. Among cytokines which were involved in plasticity of ILC1 and ILC3, only IL-23 mRNA or protein expression from tumor cells was significantly correlated with the number of ILC1 and ILC3. And the percentage of ILC3 was associated with IL-23 expression in tumor cells but not immune cells.

Based on these findings, it was suggested that the conversion of ILC1 from ILC3 in TME could be caused by IL-23 expression from tumor cells. The polarization of ILC1 into ILC3 was observed in experiment of *in vitro* co-culture model using sorted-ILC1 or total ILCs and SqCC which expresses high level of IL-23, but not in co-culture of sorted ILC1 or total ILCs and ADCs. In *in vivo* murine tumor model, tumor growth was dependent on IL-23 expression from tumor cells via IL-17 from converted ILC3 from ILC1.

In retrospective cohort using immunohistochemistry on TMA, the numbers of CD3$^-$RORγt$^+$ ILC3, IL-17 expression level, and IL-23- or IL-17RA-expressing tumor cells were more frequently observed in SqCC. These factors were also associated with short survival of patients with SqCC but not ADC.

In conclusion, these results indicate that IL-23 produced by tumor cells drives differentiation ILC1 toward ILC3 and the interaction of IL-17

expression from ILC3 and IL-17R on tumor cells promotes tumor proliferation. Therefore, the IL-23 – ILC3 – IL-17 axis affects to poor prognosis in lung cancer patients, this axis may suggest potential immunotherapy targets for patients with IL-23-producing lung cancers.

……..

Keywords: Innate lymphoid cell, plasticity, Interleukin-23, Interleukin-17, tumor microenvironment, lung cancer, human

Student Number: 2012-21730

Contents

List of Tables

List of Figures

1. Introduction

1.1 Different two subtypes of non-small cell lung cancer

Non-small cell lung cancer (NSCLC), which accounts for 85% of all lung cancers, is the leading cause of cancer-related death worldwide (1). Among NSCLCs, adenocarcinoma (ADC) and squamous cell carcinoma (SqCC) are two major histological subtypes that exhibit distinct epidemiologic, biological and genetic characteristics (2, 3). About 40% of lung cancers are ADCs. These cancers start in early versions of the cells that would normally secrete substances such as mucus (4). This type of lung cancer occurs mainly in current or former smokers, but it is also the most common type of lung cancer seen in non-smokers. It is more common in women than in men, and it is more likely to occur in younger people than other types of lung cancer (5). ADC is usually found in outer parts of the lung. Though it tends to grow slower than other types of lung cancer and is more likely to be found before it has spread, this varies from patient to patient (6). About 25% to 30% of all lung cancers are SqCC. These cancers start in early versions of squamous cells, which are flat cells that line the inside of the airways in the lungs. They are often linked to a history of smoking and tend to be found in the central part of the lungs, near a main airway (bronchus) (5). For treatment, different chemotherapeutic regimens should be administered to the two NSCLC subtypes due to their unique genetic and epigenetic profiles (7). Meanwhile, immunotherapy has recently emerged as a strong therapeutic strategy for the treatment of lung cancer (8). The responsiveness of

immunotherapy differs in the two types of NSCLCs (9, 10). The studies of the tumor microenvironment (TME) within and between ADC and SqCC remain scarce. And the differential effects in immunogenicity within ADCs and SqCC have not yet been explored. Therefore, a comprehensive understanding of the immune regulatory network in TME of each individual type of NSCLC is critical for achieving efficient and successful treatment outcomes using immune reagents.

1.2 Various strategies for tumor survival

In TME, dynamic and complex network is made up by various types of cells including malignant cells, immune cells, fibroblasts and blood vessels, which influences the development and progression of tumors and patient prognosis (**Figure 1**) (11). Thus, the comprehensive understanding of regulatory pathways for TME network is critical to establish therapeutic strategies for malignant tumors. During crosstalk between tumor and stromal cells in TME, tumor cells employ diverse strategies that help to facilitate tumor growth and development into the life-threatening entities, including cytokine and chemokine production, accumulation of genetic and/or epigenetic alteration in tumor cells, and suppression of immune system. Tumor cells use several strategies to facilitate tumor growth and development into the life-threatening entities. First, tumor cells secrets cytokine such as interleukin-8 (IL-8) to its own proliferation and survival through autocrine signaling pathways (12, 13). Second, the accumulations of genetic and/or epigenetic alterations in tumor cells not only affect to cancer development,

also to tumor cell proliferation. For example, genetic alteration of epidermal growth cell receptor (EGFR) which is most frequently observed in non-small cell lung cancer (NSCLC), lead to up-regulation of pro-oncogenic process and promote cell cycle proliferation through various intricate EGFR related signaling pathways (14). Third, Tumor cells could suppress the immune system to enhance their survival. Tumor cells escape from immune surveillance by decreasing expression of certain antigen-presenting proteins like MHC molecule at their surface or by expressing immune-editing proteins such as programmed cell death 1 ligand-1 (PD-L1) (15, 16). Forth, tumor cells cause dynamic change of conversion or differentiation of immune cells to induce suppressive phenotypes of $CD4^+$ T cells, macrophages and myeloid derived suppressive cells (MDSC) (17, 18). These cancer's self-preservation mechanisms are critical for tumor survival and have a great effect on non-malignant cells in TME.

However, it is difficult to figure out exact these tumor-survival mechanism in cancer because each tumor has different mechanisms for its survival and the consideration of dynamic effects of non-malignant cells in TME. For this reason, there is little knowledge about tumor-survival strategies and the needs of understanding of tumor survival mechanisms are increasing.

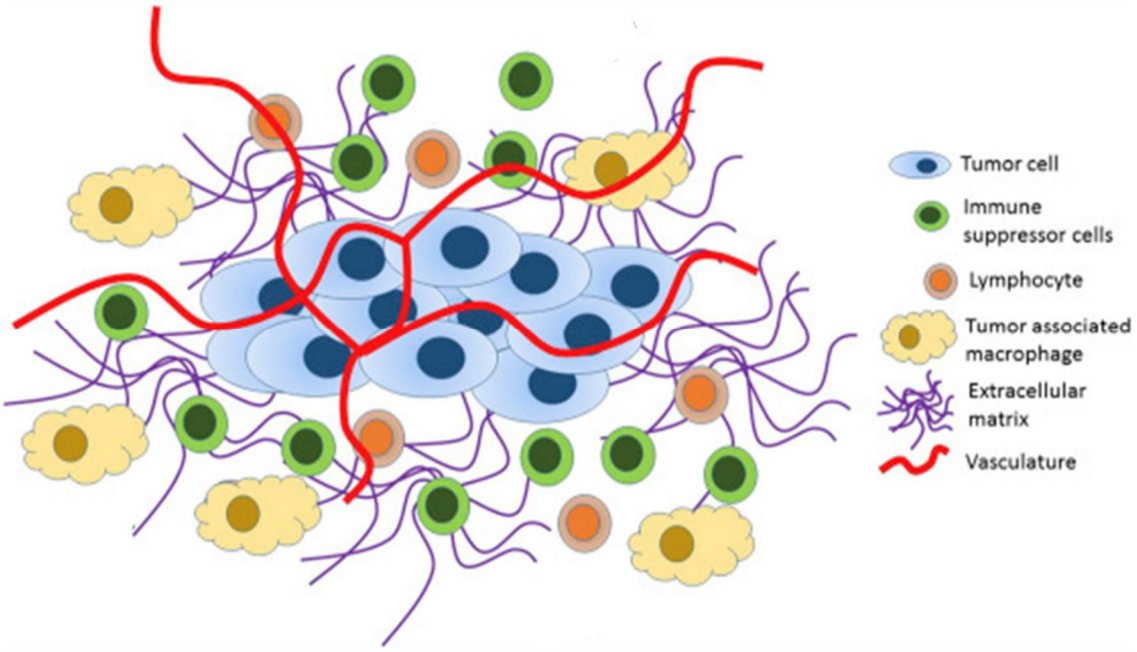
Tumor cell
Immune suppressor cells
Lymphocyte
Tumor associated macrophage
Extracellular matrix
Vasculature

Figure 1. Tumor microenvironment

A schematic representation of the tumor microenvironment. Tumor microenvironment is a complex network composed of extracellular matrix (ECM), stromal cells (fibroblasts, endothelial cells and pericytes) and various kinds of immune cells (T cells, B cells, natural killer cells, innate lymphoid cells, dendritic cells, macrophages and myeloid-derived suppressor cells).

1.3 IL-17 pathway in tumor microenvironment

IL-17 is isolated as a CD4-specific transcript from a rodent cDNA library (19, 20). IL-17 is the founding member of a new cytokine family composed of six cytokines and five receptors (20-24). IL-17 is generated by various immune cells, including CD4+ T helper (Th) cells, γδ T cells, natural killer T (NKT) cells, NK cells, and Group 3 ILCs, thereby regulating various immune responses in autoimmune diseases, cancer, infection, and transplantation (25). Regarding the functional roles of IL-17 in the TME, emerging evidence has demonstrated that IL-17 has pro-tumor effects by regulating immune evasion, angiogenesis, and tumor proliferation, although anti-tumor effects have also been reported (25). So IL-17 is one of factors involved in antitumor and pro-tumor immunity and need to be studied in depth to minimize their pro-tumor effects and enhance the antitumor effects. The dynamic and complex TME is composed of various types of cytokines, including IL-17 and immune cells, resulting in the regulation of tumor development and progression (26). The cellular network and underlying molecular mechanisms that regulate the IL-17-IL-17 receptor (R) axis in tumor progression are largely unclear due to the complexity of the TME. Many factors released by tumor cells and by standing stromal cells, such as TGF-β, IL-6, IL-21, IL-23, IL-1 β and TNF-α can play major roles in the induction of IL-17 secreting cells (27-29). But the study of existence and contribution of these factors in lung cancer is scarce. Furthermore, among IL-17-producing immune cells, the contribution of each individual cell subset to IL-17-mediated tumor

progression and its downstream mechanisms in human lung cancer remain elusive.

1.4 Innate lymphoid cells and regulation of tumor immunity

ILCs are a distinct cell type in the innate immune system that have a lymphoid morphology but lack the expression of somatically rearranged antigen receptors and cell-surface markers for myeloid or dendritic cells (DCs) (30). ILCs has become an important population in innate immunity and have a critical roles in tissue remodeling (31). Similarly to NK cells and lymphoid tissue-inducer (LTi) cells, this population depends on common cytokine receptor γ-chain and the transcriptional repressor inhibitor of DNA binding 2 (ID2) for their development (32, 33). These populations also depend on signaling of IL-7 receptor subunit α (IL-7R α) for their development and maintenance. ILCs are divided into three distinct subclasses (ILC1, ILC2, and ILC3) based on their cytokine profiles and set of expressed transcription factors (**Figure 2**) (34). Group 1 ILCs (ILC1) express T-bet and produce interferon (IFN)-γ. Group 2 ILCs (ILC2) produce IL-4, IL-5, IL-9, and IL-13 and express GATA3, and group 3 ILCs (ILC3) produce IL-22 alone or in combination with IL-17A and express ROR γ t compatible with T-helper cells fates. ILCs play a critical role in regulating the immune responses in various immune-related diseases, including colitis, asthma, and obesity-induced glucose intolerance (34-36). Experimental evidence suggests that ILCs act as a double-edged sword in tumor progression and regression (37). ILC1 have multiple functions such as cytotoxicity, macrophage activation, chronic viral

infection and cancer (38, 39). ILC1 produce cytokines upon stimulation by IL-12 or IL-18. The function of ILC1 in TME has been reported as antitumor factor by secretion of IFN-r, activation of cytotoxic CD8 T cells and inhibition of macrophage differentiation, such as TSLP, IL-25 and IL-33 (40-46). On the other hand, ILC2 are dependent on epithelial cell derived cytokines to regulate responses during infection or inflammation (47). It is well known that ILC2 have an effect on the anthelminthic inflammation (42). In TME, ILC2 involved in establishment of immunosuppressive environment by increased numbers of Treg and MDSC by expressing IL5 and IL-13 (48). By contrast, ILC3 has both pro- and anti-tumor effects (49). Some studies suggested that ILC3 mediated IL-17 promotes tumorigenesis by inducing angiogenesis or inhibition of tumor cell death (50-53), other studies insisted ILC3 controls tumor growth by activating or recruiting NK cells, T reg and neutrophils in TME (54, 55). With respect to ILC in human lung cancer, NCR^{+}ILC3 cells have been detected at the edge of the tumor-associated tertiary lymphoid structure in NSCLCs from patients (49). However, the functional roles of ILCs in human lung cancers remain unclear.

As mentioned before, ILC and Th cells express identical sets of effector cytokines and master transcriptional factors (56), which suggests that these two cell subsets share common regulatory mechanisms for their plasticity. The switches and trans-differentiation of Th cells have been demonstrated both in vitro and in vivo (57). Similar to Th cells, distinct stimulations regulate the plasticity between ILC1 and ILC3 in vitro and in the specific microenvironment of the intestine in patients with Crohn's disease (57). The

plasticity of ILC3 subsets have suggested by various reports. Firstly, data showing that culture of human ILC3 in IL-2 led to the emergence of IFN-g-producing cells, which was accompanied by decreased RORC expression (54). In addition, data from genetic fate mapping studies showed, that NKp46+ ILC3 can downregulate RORγt expression (58). In intestine, ILC1 differentiated to ILC3 in the presence of IL-2, IL-23, IL-1β dependent on RORγt. The plasticity of ILCs in the TME has not yet been reported. Moreover, whether ILC plasticity in the TME affects IL-17-mediated regulation of the TME and the prognosis of patients with cancer remains unknown.

To address these issues, I investigated whether the IL-17-IL-17R axis contributes to tumor progression of two histological types of NSCLCs and whether the plasticity of ILC affects IL-17-mediated regulation of the TME. I also analyzed the prognostic effects of ILC3 on patients with SqCCs and ADCs of the lung.

I found that the IL-17-IL-17R axis is activated in SqCCs but not ADCs, and IL-23-producing SqCCs promotes IL-17-mediated tumor progression by converting ILC1 into ILC3 in the TME, thereby shortening patient survival.

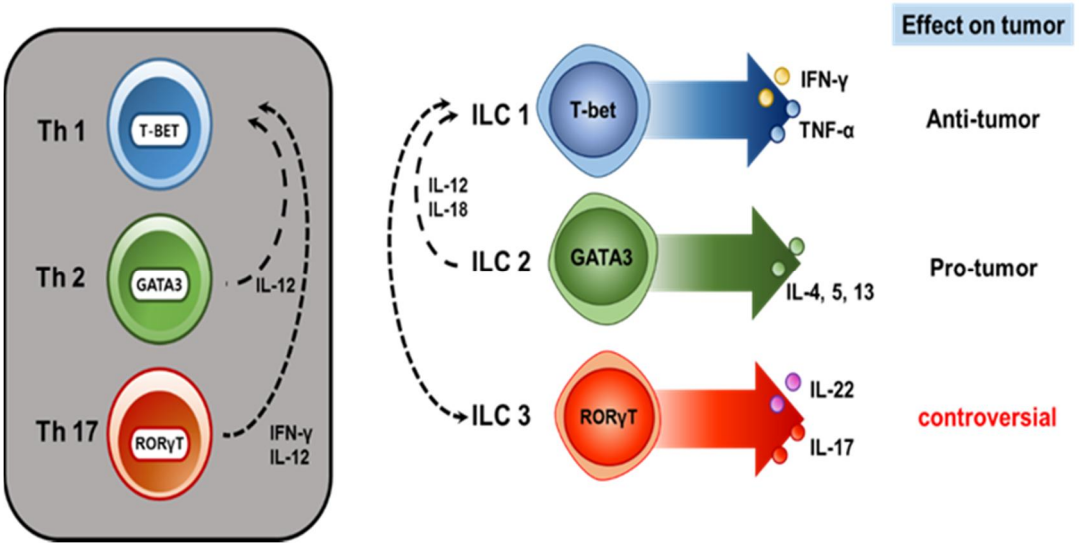
Th 1
T-BET
Th 2
GATA3
IL-12
Th 17
RORγT
IFN-γ
IL-12
Effect on tumor
ILC 1
T-bet
IFN-γ
TNF-α
Anti-tumor
IL-12
IL-18
ILC 2
GATA3
IL-4, 5, 13
Pro-tumor
ILC 3
RORγT
IL-22
IL-17
controversial

Figure 2. Characteristics and effect on tumor of innate lymphoid cell subsets

ILCs divided into three subsets analogous to T helper lymphocytes. ILC1 cells express the transcription factor T-bet and produce IFN-γ and TNF-α like Th 1 cells. ILC2 cells secret IL-4, IL-5 and IL-13 and display a GATA3 mirror to Th 2 cells. ILC3 cells have shown to be associated with IL-17 and IL-22 production, as well as RORγt transcription factor expression, characteristic of Th17 cells. ILC has three subsets, mirror to helper T cell subsets. ILC1 has anti-tumor effect, on the contrary, ILC2 may contribute to tumor progression. ILC3 may promote tumor progression and regression according to the phase of responses and site-dependent manner.

2. Materials and methods

2.1 The cohorts of patients with NSCLC

Fresh tumor and non-tumor lung tissues (NTLT) were obtained from 80 patients who underwent surgery for NSCLCs (40 ADCs and 40 SqCCs) without neoadjuvant chemotherapy or any other lung disease at the Department of Thoracic Surgery of Seoul National University Hospital (SNUH; Seoul, Korea). All patients provided written informed consents for this study. The baseline clinicopathologic characteristics of prospective cohort of these patients are summarized in **Table 1**. For tissue microarray analyses, tissues were collected from 875 patients who underwent surgery for pulmonary ADC (497 cases) or SqCC (378 cases) and had been followed up at SNUH from 2001 to 2012 (**Table 2**). No patients had received chemotherapy before surgery or had distant metastasis at the time of diagnosis. Clinicopathological data and pathologic tumor node metastasis staging from the 7th American Joint Committee on Cancer were obtained from medical and pathological records (Table 2). This study followed the World Medical Association Declaration of Helsinki recommendations and was approved by the Institutional Review Board of SNUH (H-1404-100-572).

2.2 Preparation of fresh tissues obtained from NSCLC patients and tissue microarray

To perform flow cytometric analysis, tumors of at least 1 cm^3 in size and matched NTLT were obtained immediately after surgical resection. Tissue

was mechanically dissociated using a blade and subsequently digested in RPMI 1640 medium (Invitrogen) supplemented with 80 U/mL DNase I, 300 U/mL collagenase I, and 60 U/mL hyaluronidase at 37°C for 30 min. The single-cell suspension was passed through a 70 μm cell strainer. After red blood cell lysis, cells were washed and used for cell sorting, RNA extraction for real-time polymerase chain reaction (PCR), and flow cytometry. In addition, a tissue microarray was constructed from 2 mm diameter cores derived from representative tumor areas of formalin-fixed paraffin-embedded (FFPE) tissue blocks.

2.3 Human and mouse lung cancer cell lines

Human lung SqCC cell lines (H1703 and SK-MES1) and ADC cell lines (H522 and A549), and mouse SqCC cell line (KLN-205) cells were purchased from the American Type Culture Collection (ATCC), while HCC-15 (human lung SqCC cell line) was purchased from Korean Cell Line Bank. H1703, HCC-15, SK-MES1, H522 and A549 cells were cultured in RPMI, whereas A549 cells were cultured in DMEM (Invitrogen) supplemented with 10% fetal bovine serum, 100 U/mL penicillin, and 100 μg/mL streptomycin in a humidified incubator at 37°C with 5% CO_2. These cell lines were regularly tested by PCR, to ensure they were Mycoplasma negative. The cell lines were authenticated by short tandem repeat DNA fingerprinting (Korean Cell line bank).

2.4 Antibodies for immune subset analysis using flow cytometry

The following antibodies were used to detect lymphocytes: anti-CD45-Alexa 700 (H130; BioLegend, San Diego, CA, USA), anti-CD3-Percp-Cy5.5 (UCTH1; BD Biosciences, Franklin Lakes, NJ, USA), anti-CD4-Alexa 488 (RPA-T4; BioLegend), anti-CD8-APC-cy7 (SK1; BioLegend), anti-CD19-BV421 (H11319; BioLegend), anti-CD56-BV605 (NCAM16.2; BD Biosciences), anti-CD25-BV711 (2A3; BD Biosciences), and anti-CD127-PE-Cy7 (A019D5; BioLegend). Representative gating strategy for lymphoid cells is summarized in **Figure 3.**

To detect myeloid cells, anti-CD45-Alexa 700, CD3-Percp-Cy5.5, CD14-Alexa 488 (MQP9; BD Biosciences), HLA-DR-BV786 (G46–6; BD Biosciences), anti-CD11c-PE-cy7 (B-ly6; BD Biosciences), anti-CD33-APC (551378; BD Biosciences), anti-CD206-PE (MMR; eBioscience, San Diego, CA, USA), anti-CD1c-APC-cy7 (L161; BioLegend), anti-CD123-BV650 (7G3; BD Biosciences), and anti-CD141-BV510 (1A4, BD Biosciences) antibodies were used. Anti-TCR γδ-FITC (B1; BD Biosciences) was purchased and CD1d/PBS57 tetramers-APC was obtained from the National Institute of Health Tetramer Core Facility (Bethesda, MD, USA). Representative gating strategy for myeloid cells is summarized in **Figure 4.**

The following antibodies were used to identify ILC subsets (**Figure 5**): anti-CD45-Percp-Cy5.5 (HI30; BD Biosciences), anti-CD3e -FITC (UCHT1; BioLegend), anti-CD11c-FITC (3.9; BioLegend), anti-CD11b-FITC (ICRF44; BioLegend), anti-CD14-FITC (HCD14; BioLegend), anti-CD19-FITC

(HIB19; BioLegend), anti-CD49b-FITC (P1E6-C5; BioLegend), anti-FcεRIα-FITC (AER-37; BioLegend), anti-CD127-Pe-cy7 (A019D5; BioLegend), anti-CD117-BV421 (104D2; BioLegend), anti-NKp44-APC (P44–8; BioLegend), and anti-ST2L-PE (B4E6; MD Bioproducts, Oakdale, MN, USA).

For intracellular staining, single-cell suspensions prepared from fresh tumor and NTLT were pre-incubated with Fc receptor blocking solution (BioLegend) to reduce nonspecific binding and subsequently stained for various markers. Cells were stained for surface antigens for 30 min at 4°C. For intracellular staining, cells were stained with anti-IL23p19-FITC (IC17161G; R&D Systems, Minneapolis, MN, USA), IL-17A-PE (512306; BioLegend), IL-22-PE (366703; BioLegend), T-bet-BV421 (4B10; BioLegend), GATA3-APC (16E10A23; Biolegend), RORγt-PE (563081; BD Bioscience), and Ki-67-FITC (11–5699–41; eBioscience) antibodies were used for human samples, while anti-mouse IL23p19- eFlour 660 (fc23cpg; eBioscience), IL-17A (TC11-18H10.1; BioLegend), T-bet-eflour 647 (4B10; BioLegend), GATA3- APC (16E10A23; BioLegend) and RORγt BV421 (Q31-378; BD Bioscience) antibodies were used for mice and fixed. An amine reactive dye (Aqua LIVE/DEAD Stain Kit; Life Technologies, Thermo Fisher Scientific, Waltham, MA, USA) was used to exclude dead cells according to the manufacturer's instructions.

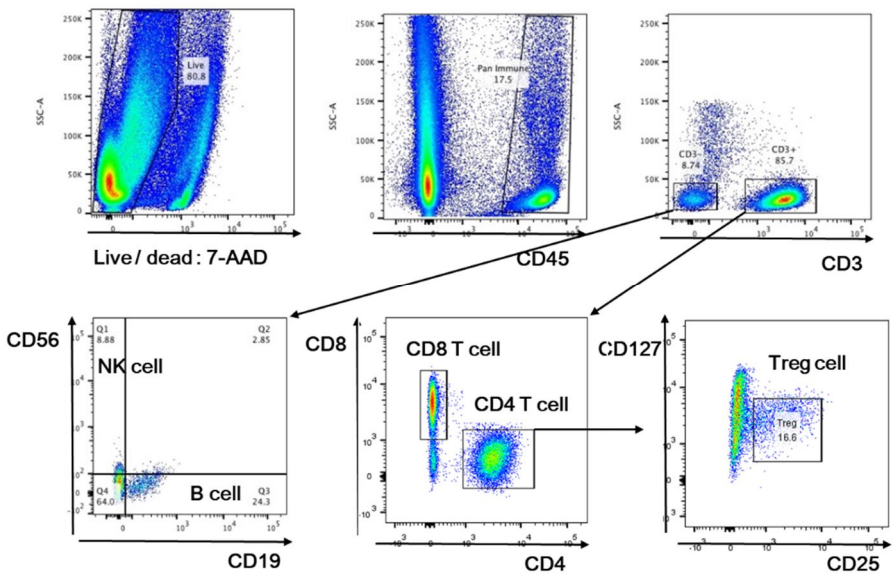

Figure 3. Gating strategy of lymphoid cells

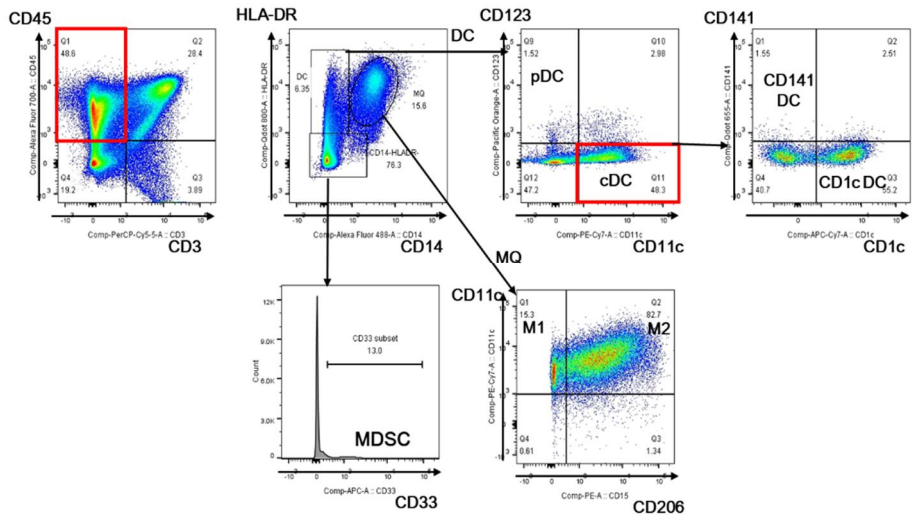

Figure 4. Gating strategy of myeloid cells

Figure 5. Gating strategy of innate lymphoid cells

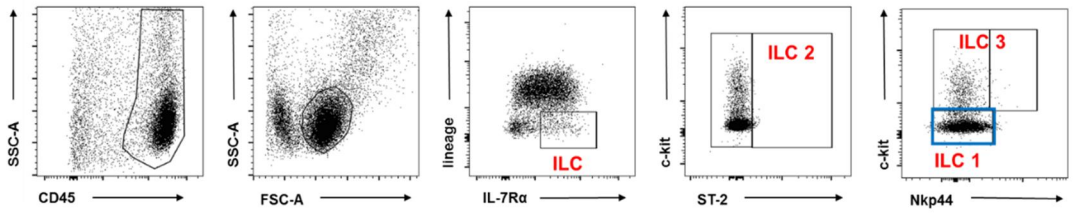

2.5 Cell sorting

To sort total ILCs using flow cytometry, suspended cells from tumor or NTLT were labeled with various antibodies, anti-CD45-Percp-Cy5.5 (HI30; BD Biosciences), anti-CD3e-FITC (UCHT1; BioLegend), anti-CD11c-FITC (3.9; BioLegend), anti-CD11b-FITC (ICRF44; BioLegend), anti-CD14-FITC (HCD14; BioLegend), anti-CD19-FITC (HIB19; BioLegend), anti-CD49b-FITC (P1E6-C5; BioLegend), anti-FcεRIα-FITC (AER-37; BioLegend), and anti-CD127-Pe-Cy7 (A019D5; BioLegend) antibodies. To sort ILC1, anti-CD117-BV421 (104D2; BioLegend) and anti-ST2L-PE (B4E6; MD Bioproducts) antibodies were used. After labeling, cells were sorted using a FACSAria (BD Biosciences) to > 95% purity. Tumor and immune cells were isolated from fresh tumor tissues using the magnetic bead sorting MidiMACS system (Miltenyi Biotec, Bergisch Gladbach, Germany) based on the binding of anti-EpCAM-APC (9C4; BioLegend) or anti-CD45-PE (555483; BD Biosciences).

2.6 Lentiviral transduction and transfection study

The recombinant lentivirus was generated by using the construct of the mouse IL23p19 open reading frame expression clone (EX-Mm12283-Lv105; GeneCopoeia, Rockville, MD, USA) and the Lenti-Pac HIV expression Packaging Kit (GeneCopoeia) according to the manufacturer's instructions. 293Ta packaging cell line was transfected overnight with the mouse IL23p19 expression clone and packaging plasmids. After 16 h, fresh medium was added to the cells and incubated overnight. On three consecutive days after

transfection, the pseudotyped virus-containing culture medium was harvested, filtered, supplemented with 8 μg/ml polybrene (Sigma-Aldrich). After KLN-205 cells were infected, stable transfected cells were selected in puromycin. Control cells were transduced with the control lentiviral vector. Fluorescence analysis or real-time PCR were performed to evaluate the IL-23 overexpression efficiency.

2.7 Mice and tumor inoculation *in vivo*

BALB/c mice were obtained from Orient Bio Inc. (Seongnam-si, Gyeonggi-do, Korea). Tumors were established by subcutaneously injecting IL-23-overexpressing KLN-205 or control KLN-205 (transduced with empty vector) or wild type KLN-205 cells (2×10^5 cells per injection) into the flanks of 6- to 8-week-old BALB/c mice in the presence or absence of the indicated dose of control Ig (eBRG1; eBioscience) or anti-IL23p19 antibody (clone 16-7232-81; eBioscience). These antibodies were administered on the first day of tumor injection and repeatedly every 4 days. Tumor growth was estimated by measuring tumor diameters using a digital caliper. On day 21, mice were euthanized and tumors were harvested for further analysis. This study was approved by Institutional Animal Care and Use Committee of Clinical Research Institute, SNUH and Institutional Biosafety Committee of SNU. This facility was accredited by the Association for the Assessment and Accreditation of Laboratory Animal Care International.

2.8 Immunohistochemistry

FFPE tissue blocks were cut into slices of 4 μm thickness and subjected to immunohistochemistry to analyze the expression of IL-17RA (clone 49M4D2; 1:100, Novus Biologicals, Littleton, CO, USA) and IL-23 (clone ab45420; 1:200, Abcam, Cambridge, United Kingdom). All immunohistochemistry studies were performed using the Ventana Benchmark XT automated staining system (Ventana Medical Systems, Tucson, AZ, USA) according to the manufacturer's protocol. Double immunohistochemistry staining was performed with primary antibodies against CD3 (F7.2.38; Dako, Carpinteria, CA, USA), CD20 (L26; Dako), and RORγT (ab80690; Abcam). After overnight incubation, slides were washed and incubated with a horseradish peroxidase-linker antibody and an alkaline phosphatase-linker antibody. Detection was performed with 3, 3-diaminobenzidine (DAB, brown chromogen) and Vector Blue. The percentages of stained tumor cells and the pattern of their staining were assessed; 5% of membranous or cytoplasmic staining was considered a cut-off point for positive IL-17RA and IL-23 expression. ILC3 was defined as cells expressing RORγT in the absence of CD3 and CD20 expression. The numbers of ILC3 were measured in each core of the tissue microarray.

2.9 Immunofluorescence

Frozen sections of tumor tissues were attached to coverslips, fixed in acetone solution for 15 min, and washed three times with phosphate-buffered saline (PBS). Sectioned tissues were blocked with 5% bovine serum albumin in PBS for 30 min at room temperature. After washing with PBS, sectioned

tissues were incubated at room temperature for 1 h with following antibodies: anti-CD3-FITC (UCHT1; BioLegend), anti-RORγT- Alexa Fluor 647 (563620, BD Biosciences), and anti-CD117-DAPI (104D2; BioLegend). Sectioned tissues were washed, covered with coverslips, and examined under a fluorescence microscope.

2.10 Quantitative real-time PCR

RNA was isolated from sorted tumor cells and immune cells using TRIzol (Life Technologies, Carlsbad, CA, USA) and reverse-transcribed into cDNA using RNAM-MLV Reverse Transcriptase (Promega, Madison, WI, USA) according to the manufacturer's protocol. Gene-specific PCR products were measured using an Applied Biosystems 7500 Sequence Detection System (PerkinElmer Biosystems, Foster City, CA, USA). The sequences of primers were summarized in **Table 3**. Relative gene expression was normalized to that of glyceraldehyde 3-phosphate dehydrogenase (GAPDH; Hs02758991_g1).

2. 11 Proliferation assay

Lung SqCC cell lines and tumor cells isolated from SqCC patients were seeded at a density of 5×10^4 cells/well in 48-well plates. Cells were grown overnight, and the medium was replaced with maintenance medium containing the desired concentrations of cytokines or antibodies or medium. Cell viability was assessed after 96 h based on cell number and the Ki-67 index.

2. 12 *In vitro* culture of ILCs

Total ILCs or ILC1 were isolated from fresh tissues of ADCs or SqCCs, sorted, plated in a 96-well plate (2×10^4 cells/well), and stimulated with recombinant IL-2 (10 U/mL; Novartis, Basel, Switzerland) and IL-23 (50 ng/mL; R&D Systems) for 5 days.

2. 13 Co-culture experiments using ILCs

Tumor cell lines (4×10^4 cells/well), or tumor cells isolated from fresh tissues of ADCs or SqCCs (5×10^4 cells/well) were plated in a 48-well plate. After 24 h, sorted total ILCs or ILC1 (3×10^4 cells/well) from NTLT or NSCLCs were added and co-cultured for an additional 5 days in the presence of an anti-IL-23-neutralizing (HNU2319; eBioscience), anti-IL-1β-neutralizing (B122; eBioscience), anti-IL-17-neutralizing (eBio64CAP17; eBioscience), or anti-IL-22-neutralizing (22URTI; eBioscience) antibody. During co-culture, adherent and non-adherent cells were obtained after stimulation with 10 ng/mL PMA and 0.5 μg/mL ionomycin for 4 h. Non-adherent cells were stained for 30 min using ILC panel antibodies, anti-IL-17, or anti-IL-22 antibody, while adherent cells were treated with trypsin/EDTA, washed, and stained with anti-Ki-67 antibody or subjected to RNA isolation for RT-PCR. The amounts of IL-17 were measured in culture supernatants using enzyme-linked immunosorbent assay (ELISA) kit (eBioscience)

2. 14 RNAseq analyses

$CD3^+$ T cells were obtained from fresh tumor tissues and NTLT of ADCs and SqCCs and sorted using flow cytometry. Total RNA was isolated from sorted $CD3^+$ T cells using the RNeasy Mini Kit (Qiagen, Hilden, Germany). RNA quality and quantity were determined on a Nanodrop (Nanodrop Technologies, Wilmington, DE, USA) and the Agilent 2100 Bioanalyzer (Agilent Technologies, Palo Alto, CA, USA). RNA-seq analyses were performed at Theragen Bio Institute (Suwon-si, Gyeonggi-do, Korea). Raw read filtering, gene normalization, and differentially expressed gene analyses were performed as previously described (59).

2. 15 TCGA data analyses

Gene expression data for pulmonary NSCLC were obtained from TCGA, which is available through the cBio Cancer Genomics Portal. Clustering-based analyses were performed for cell proliferation, migration, and angiogenesis. Each gene cluster was defined as “angiogenesis; GO: 0001525”, “epithelial cell proliferation; GO: 0050673”, or “positive regulation of epithelial cell migration; GO: 0010634” according to Gene Ontology annotation. Comparisons were made between tumors with and without *IL17A* expression (mRNA level > 0). Analyses were performed using the R language and core packages (gplots and RColorBrewer).

2. 16 Statistics

Comparisons between variables were performed using the χ^2 test, Student's t-test, or paired t-test. Survival analyses were performed using the Kaplan-Meier method with the log-rank test. Two-sided P values less than 0.05 were considered statistically significant in all analyses. Progression-free survival was measured from the date of surgery to that of recurrent or metastatic disease occurrence. Prism GraphPad software (San Diego, CA, USA) was used for most of statistical analyses. And the genomic analysis with data presentation were performed using the R statistical package 3.4.2

Table 1. Patient Characteristics of prospective cohort of NSCLC

	SqCC (n=40)	ADC (n=40)
Variables	N (range or %)	N (range or %)
Age (years)		
Median (range)	69.5 (56–82)	62.4 (48-88)
Gender		
Men	38 (95.0)	21 (52.5)
Women	2 (5.0)	19 (47.5)
Smoking statue		
Never	3 (7.5)	18 (45.0)
Ever	37 (92.5)	22 (55.0)
Smoking PY	43.5 (0.5-135)	30.6 (1-80)
Tumor size		
Median (range)	3.97 (1.5-7.5)	3.46(2.2-5.5)
pN stage		
N0	22 (55.0)	36 (90.0)
N1-2	18 (45.0)	4 (10.0)
pStage		
I	16 (40.0)	30 (75.0)
II	15 (37.5)	6 (15.0)
III	9 (22.5)	3 (7.5)
IV	0	1 (2.5)
EGFR mutation		
No	38 (95.0)	21 (52.5)
Yes	0 (0)	18 (45.0)
Unknown	2 (5.0)	1 (2.5)

Abbreviations; ADC, adenocarcinoma; NSCLC, non-small cell lung cancer; PY, pack-year; SqCC, squamous cell carcinoma

Table 2. Patient Characteristics of retrospective cohort of NSCLC

	SqCC (n=378)	ADC (n=497)
Variables	N (range or %)	N (range or %)
Age (years)		
Median (range)	63.8 (46–87)	66.4 (45-83)
Gender		
Men	360 (95.2)	231 (46.5)
Women	18 (4.8)	266 (53.5)
Smoking statue		
Never	22 (5.8)	299 (60.2)
Ever	356 (94.2)	198 (39.8)
Tumor size		
≤ 3cm	214 (56.6)	296 (59.6)
> 3cm	164 (43.4)	201 (40.4)
pN stage		
N0	230 (60.8)	367 (73.8)
N1-2	148 (39.2)	130 (26.2)
pStage		
I	224 (59.3)	342 (68.8)
II	74 (19.6)	46 (9.3)
III	80 (21.1)	109 (21.9)

Abbreviations; ADC, adenocarcinoma; NSCLC, non-small cell lung cancer; SqCC, squamous cell carcinoma

Table 3. The list of primers used for quantitative real-time PCR

Primers		
CCNB1	Forward	5'-GCT GCT ACC GTA GAA ATG GAA AGT G-3'
	Reverse	5'-GCC ACA GTG AGG CTA GGC CG-3'
CCNA2	Forward	5'-GGA AAA AGT CAC TTA AGC TAA CTA G-3'
	Reverse	5'- CAA GTA TCC CGC GAC TAT TGA AAT G-3'
CDC25C	Forward	5'-AGA GGG AGA GCC AAT GAT GCG C-3'
	Reverse	5'-TGA CCA TTC AAA CCT TCC GCC AG-3'
CDC7	Forward	5'-AGT GCC TAA CAG TGG CTG G-3'
	Reverse	5'-CAC GGT GAA CAA TAC CAA ACT GA-3'
Cks2	Forward	5'-ACC GGC ATG TTA TGT TAC CC-3'
	Reverse	5'-TGT GGT TCT GGC TCA TGA AT-3'
IL17A	Forward	5'-CGC AAT GAG GAC CCT GAG AG-3'
	Reverse	5'-GCC CAC GGA CAC CAG TAT C-3'
IL22	Forward	5'-GCT TGA CAA GTC CAA CTT CCA-3'
	Reverse	5'-GCT CAC TCA TAC TGA CTC CGT G-3'
IL1B	Forward	5'-GCA AGG GCT TCA GGC AGG CCG CG-3'
	Reverse	5'-GGT CAT TCT CCT GGA AGG TCT GTG GGC-3'
IL23p19	Forward	5'-CTC TGC TCC CTG ATA GCC CT-3'
	Reverse	5'-TGC GAA GGA TTT TGA AGC GG-3'
IL12p35	Forward	5'-GCT CCA GAA GGC CAG ACA AA-3'
	Reverse	5'-GCC AGG CAA CTC CCA TTA GT-3'
IL18	Forward	5'-GCT TGA ATC TAA ATT ATC AGT C-3'
	Reverse	5'-CAA ATT GCA TCT TAT TAT CAT G-3'
IL17RA	Forward	5'-ATC CTG CTG GTG GGC TCC GT-3'
	Reverse	5'-ACG TAG AGG GGG TGG TCG GC-3'
IL22R1	Forward	5'- CTC CAC AGC GGC ATA GCC T-3'
	Reverse	5'- ACA TGC AGC TTC CAG CTG G -3'

3. Results

3.1 The IL-17-IL-17 receptor axis is enhanced in pulmonary SqCCs but not ADCs

The opposite views of the role of IL-17 in malignancy has been reported. So I investigated the differential effects of the IL-17-IL-17R axis on two major types of NSCLC: SqCCs and ADCs, I estimated the expression level of IL-17R in tumor cells and the *IL17* transcript level in $CD45^+$ immune cells. I isolated $CD45^+$ immune and $CD45^-$ $EpCAM^+$ tumor cells from 80 cases of NSCLCs (40 cases of SqCCs and 40 cases of ADCs) freshly obtained from patients who underwent surgery. The transcriptional levels of *IL17RA* in tumor cells were higher in SqCCs and the SqCC cell lines (SK-MES, H1703 and HCC15) than in ADCs and the ADC cell lines (A549 and H522), respectively (**Figure 6A and 6B**). In retrospective cohort, SqCCs exhibited higher percentages of IL-17R-positive tumor cells (378 cases of SqCCs and 497 cases of ADCs) and higher expression of the *IL17* transcript in $CD45^+$ immune cells freshly obtained from tumors than ADCs (**Figure 6C and 6D**). Moreover, the expression of the *IL17* transcript in $CD45^+$ immune cells was higher in SqCCs with a high T stage (tumor size > 3cm) than in those with a low T stage (tumor size < 3cm), whereas ADCs exhibited similar expression levels of *IL17* in the two groups (**Figure 6E**). Tumor size is one of prognostic factor in patients, so the correlation of *IL17* expression in immune cells and tumor size of SqCC indicates IL-17 play a role in tumor progression.

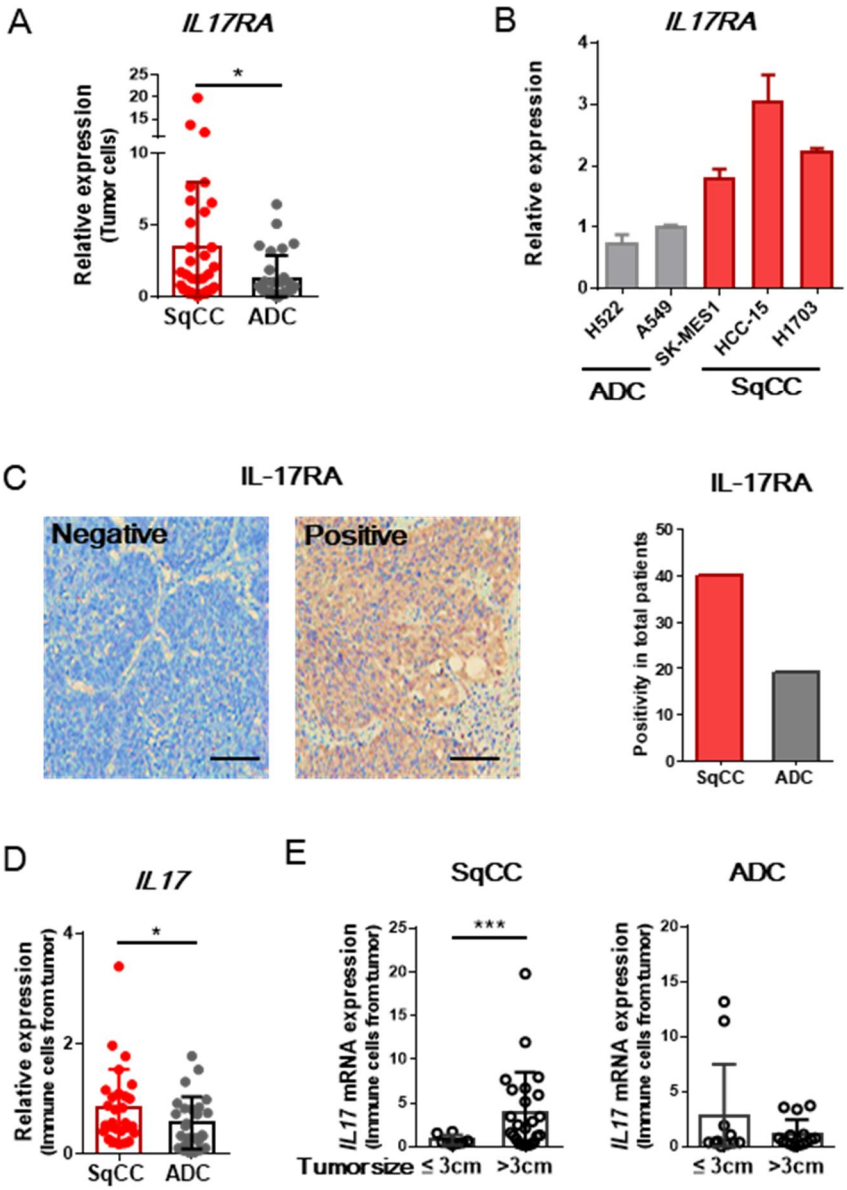
A
IL17RA
Relative expression (Tumor cells)
25
20
15
10
5
0
*
SqCC
ADC
B
IL17RA
Relative expression
4
3
2
1
0
H522
A549
SK-MES1
HCC-15
H1703
ADC
SqCC
C
IL-17RA
Negative
Positive
IL-17RA
Positivity in total patients
50
40
30
20
10
0
SqCC
ADC
D
IL17
Relative expression (Immune cells from tumor)
4
2
0
*
SqCC
ADC
E
SqCC
IL17 mRNA expression (Immune cells from tumor)
25
20
15
10
5
0
***
Tumor size ≤ 3cm
>3cm
ADC
IL17 mRNA expression (Immune cells from tumor)
20
15
10
5
0
≤ 3cm
>3cm

Figure 6. The IL-17–IL-17R receptor axis is enhanced in pulmonary SqCC rather than ADC

(**A**) Expression levels of the *IL17RA* transcript were measured in tumor cells of prospective cohorts of patients with squamous cell carcinomas (SqCCs) and adenocarcinomas (ADCs) (n = 80). (**B**) Levels of the *IL17RA* transcript in the SqCC cell lines (SK-MES1, HCC-15 and H1703) and ADC cell lines (H522 and A549). Data are presented as the mean ± SEM. (**C**) The percentages of IL-17RA-expressing tumor cells in retrospective cohort were estimated using immunohistochemistry (n = 875). Representative image of IL-17RA expression in non-small cell lung cancers (NSCLCs). Scale bars, 200 μm. (**D** and **E**) Expression levels of the *IL17* transcript were measured in $CD45^+$ immune cells freshly isolated from SqCCs and ADCs in prospective cohort (**D**), which are presented according to tumor size (**E**).

3.2 IL-17-IL-17R axis is associated with short survival of SqCC patients

Next, I analyzed The Cancer Genome Atlas (TCGA) data on the functional effects of IL-17 on angiogenesis, cell migration, and proliferation of tumor cells in NSCLCs (**Figure 7A**) (60). A heat map of proliferation-related genes revealed a clear difference in the expression patterns of *IL17*^{hi} and *IL17*^{low} NSCLCs. The expression levels of proliferation-promoting genes, such as *CCNA2, CCNB, Csk2, CDC7,* and *CDC25C*, were significantly higher in *IL17*^{hi} NSCLCs than *IL17*^{low} NSCLCs on TCGA data (**Figure 7B**). Furthermore, SqCCs expressed higher levels of these proliferation-related markers than ADCs in prospective cohort (**Figure 7C**). To evaluate IL-17 effect on tumor cell proliferation, *in vitro* culture of SqCC cell line showed that recombinant IL-17 treatment increased the Ki-67 index and the numbers of SK-MES1 cells (**Figure 8A and 8B**). These findings suggest that IL-17-mediated proliferation contributes more to the tumor progression of SqCCs than ADCs. Consistent with this hypothesis, the progression free survival of patients with IL-17R^{+} or IL-17^{hi} SqCC was significantly lower than that of those with IL-17R^{-} SqCC or IL-17^{low} SqCC, whereas patients with ADC showed similar progression-free survival regardless of IL-17R or IL-17 expression level in TME (**Figure 8C and 8D**). Together, these findings suggest that the IL-17-IL-17R axis is involved in tumor progression of pulmonary SqCCs but not ADCs.

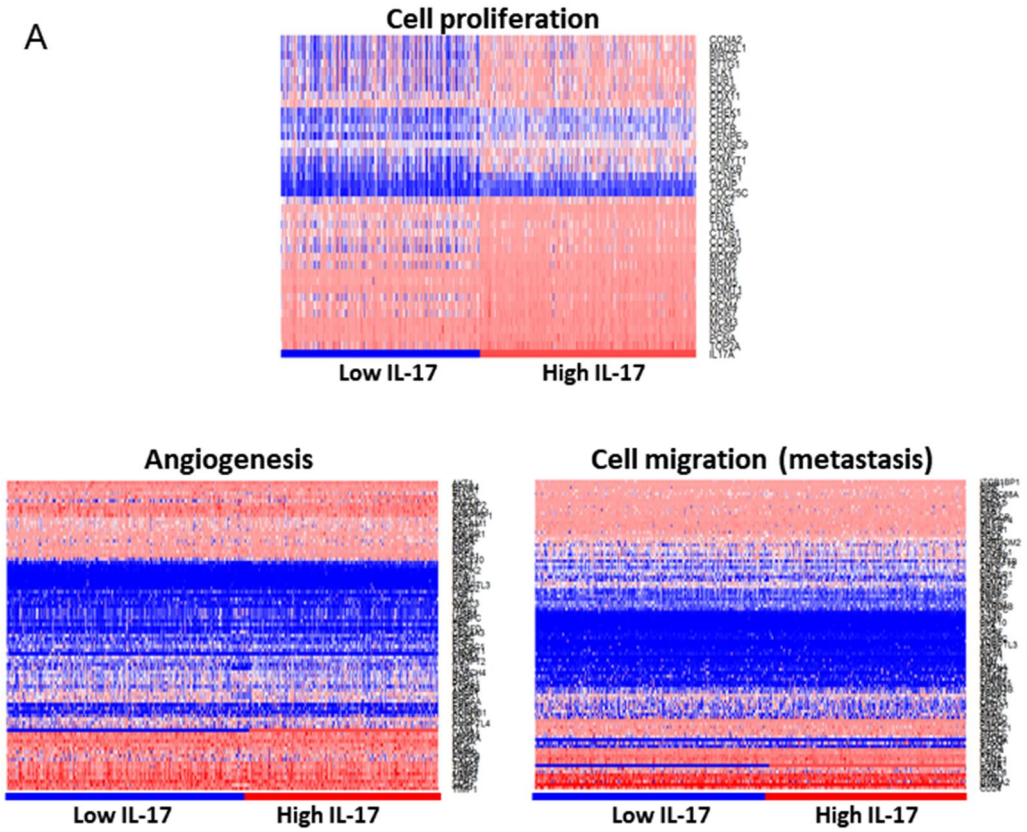
A
Cell proliferation
Low IL-17
High IL-17
Angiogenesis
Low IL-17
High IL-17
Cell migration (metastasis)
Low IL-17
High IL-17
B
CDC7
CCNA2
Cks2
CCNB1
CDC25c
IL17A low high
C
Relative expression
60
40
20
0
*
*
*
*
*
SqCC
ADC
CCNA2
CCNB1
Cks 2
CDC7
CDC25c

Figure 7. The IL-17–IL-17R receptor axis contributes to tumor progression of pulmonary SqCC

(**A**) Expression levels of cell proliferation-, cell angiogenesis- and cell migration-related molecules of IL-17^{high} versus IL-17^{low} NSCLCs were analyzed using data from TCGA lung NSCLC cohort (*n* =1097). (**B**) Expression levels of representative cell proliferation-related genes according to IL17 expression using data from TCGA lung NSCLC cohort. (**C**) Expression levels of proliferation-related molecules were measured in tumor cells freshly isolated from SqCCs and ADCs.

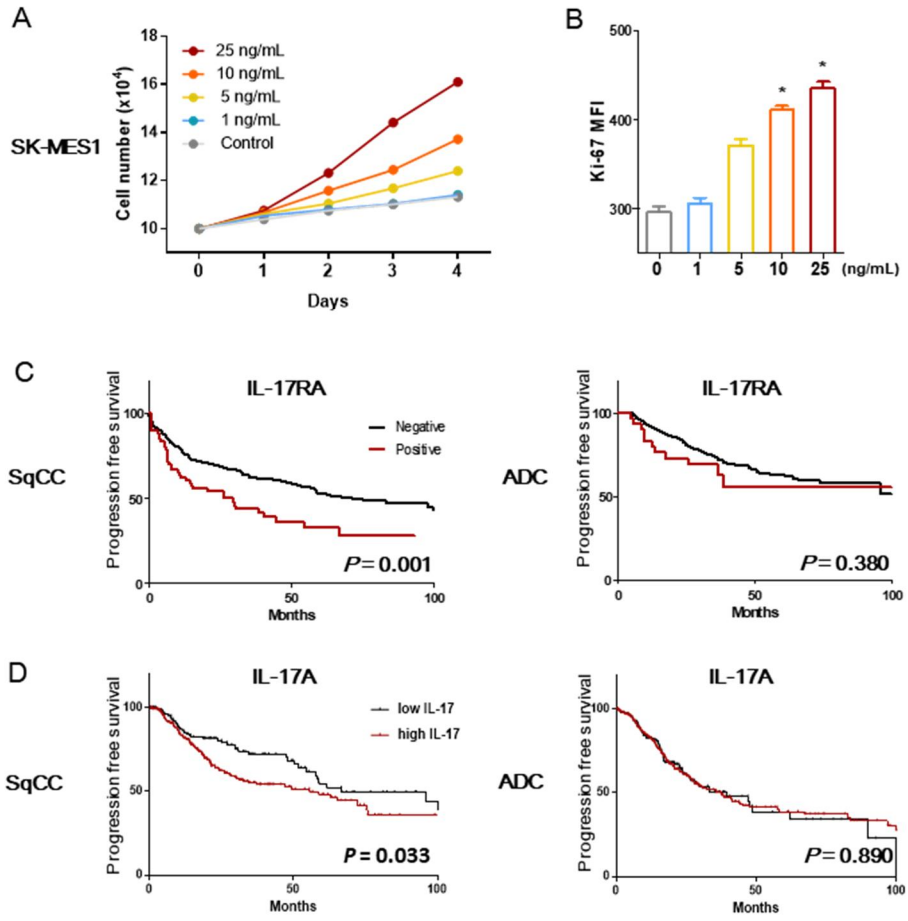
A
SK-MES1
Cell number (x10⁴)
25 ng/mL
10 ng/mL
5 ng/mL
1 ng/mL
Control
Days
B
Ki-67 MFI
(ng/mL)
C
SqCC
IL-17RA
Negative
Positive
P = 0.001
Progression free survival
Months
ADC
IL-17RA
P = 0.380
D
SqCC
IL-17A
low IL-17
high IL-17
P = 0.033
ADC
IL-17A
P = 0.890

Figure 8. The IL-17–IL-17R receptor axis is associated with tumor cell proliferation and poor prognostic factor in pulmonary SqCC

(**A** and **B**) Cell numbers (**A**) and the expression levels of Ki-67 (**B**) in SK-MES1 cells were measured after incubation with recombinant IL-17 at the indicated concentrations for 96 h. (**C** and **D**) Progression-free survival of patients with SqCC or ADC was plotted using Kaplan-Meier analyses with the log-rank test according to the IL-17RA or IL-17 expression in retrospective cohort, which was estimated using IHC.

3.3 Higher numbers of ILC3 among IL-17-producing immune cells in SqCCs

To investigate the mechanism by which SqCCs exhibit IL-17-mediated proliferation compared to ADCs, I estimated the percentages of IL-17-producing immune cell subsets in SqCCs and ADCs, because various types of immune cells produce IL-17 during regulation of the immune response and inflammation (61, 62). Flow cytometric analyses revealed that the percentages of IL-17$^+$ ILCs were higher in SqCCs than ADCs, whereas those of IL-17-expresssing lineage$^+$, CD4$^+$ T, γδ T, and NKT cells, were similar (**Figure 9A**). Moreover, a transcriptome assay revealed that CD3$^+$ T cells from SqCCs and ADCs expressed similar expression levels of various cytokines including *IL17* and *IL23p19* (**Figure 9B**). These findings suggest that IL-17-producing ILCs regulate the TME of SqCCs but not ADCs. To explore individual ILC subset further, I identified Lin$^-$CD117$^-$ST2$^-$NKp44$^-$ ILC1 by excluding NK cells based on CD49a expression, Lin$^-$ST2$^+$ c-kit$^-$ ILC2, and Lin$^-$ST2$^-$ c-kit$^+$ ILC3 in TME, which expressed their signature transcription factors and cytokines, respectively (**Figure 9C and 9D**). SqCCs exhibited a reduction in the percentage of ILC1 but an increase in both NKp44$^+$ and NKp44$^-$ ILC3 compared to NTLT in all cases of prospective cohort. However, the percentages of total ILC and ILC2 were similar in the two histological types of NSCLCs and NTLT (**Figure 10A and 10B**). Fluorescence microscopy revealed more ILC3 in the intra-tumor areas of SqCCs than ADCs (**Figure 10C and 10D**). These findings indicate that the number of ILC3 were higher in SqCC than ADCs.

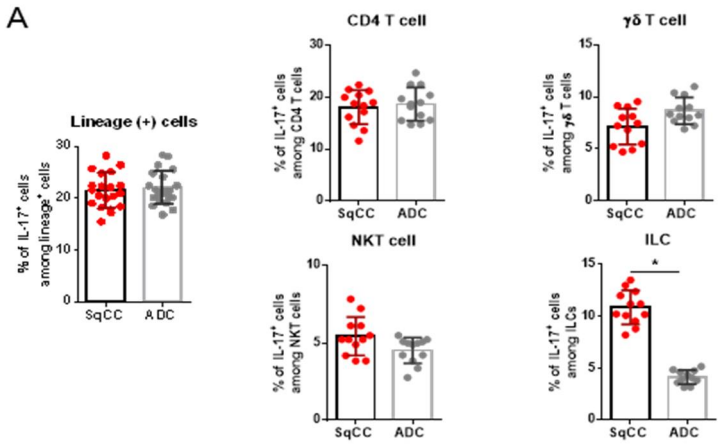
A
Lineage (+) cells
% of IL-17+ cells among lineage+ cells
SqCC
ADC
CD4 T cell
% of IL-17+ cells among CD4 T cells
γδ T cell
% of IL-17+ cells among γδ T cells
NKT cell
% of IL-17+ cells among NKT cells
ILC
% of IL-17+ cells among ILCs
*

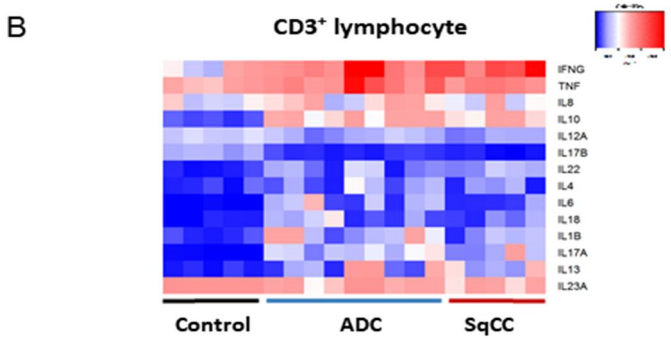
B
CD3+ lymphocyte
IFNG
TNF
IL8
IL10
IL12A
IL17B
IL22
IL4
IL6
IL18
IL1B
IL17A
IL13
IL23A
Control
ADC
SqCC

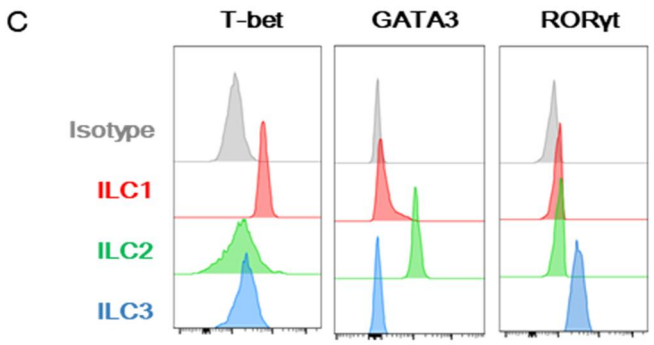
C
T-bet
GATA3
RORγt
Isotype
ILC1
ILC2
ILC3

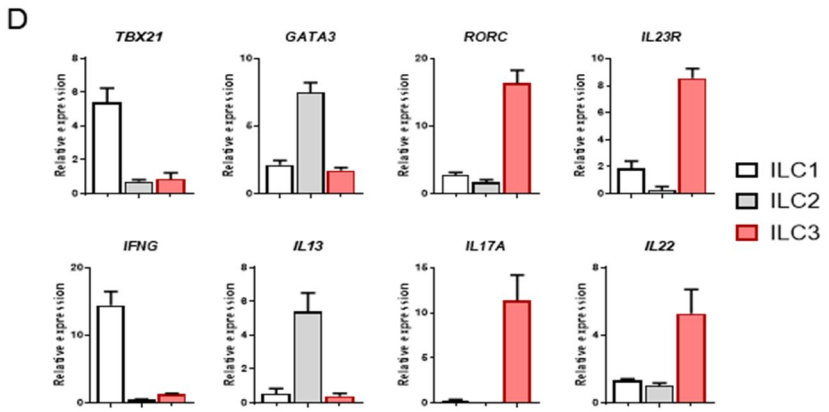
D
TBX21
GATA3
RORC
IL23R
IFNG
IL13
IL17A
IL22
Relative expression
ILC1
ILC2
ILC3

Figure 9. IL-17$^+$ ILCs were higher in SqCCs than ADCs among IL-17 producing immune cells and characterstics of ILC subsets in TME

(**A**) The percentages of IL-17-expressing immune cell subsets were estimated in the TME of SqCCs and ADCs in prospective cohort. (**B**) Heat map of the expression of various cytokines analyzed in CD3$^+$ T cells from SqCCs and ADCs using the transcriptome. (**C**) Flow cytometry analysis of the expression of T-Bet, GATA3 and RORγt in ILC subsets. (**D**) Expression of *TBX21, GATA3, RORC, IL23R, IFNG, IL13, IL17A* and *IL22* in ILC populations.

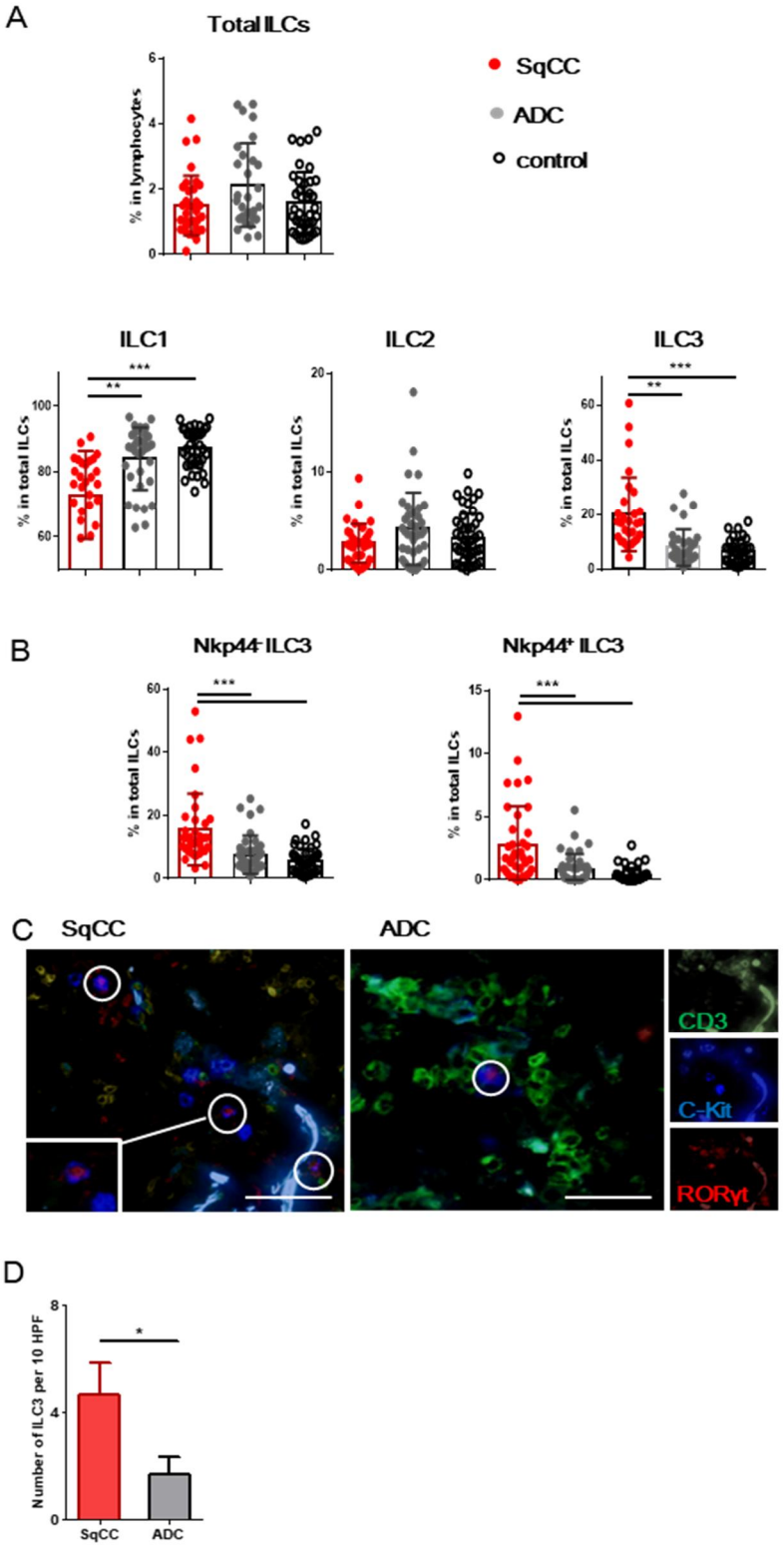
A
Total ILCs
% in lymphocytes
SqCC
ADC
control
ILC1
ILC2
ILC3
% in total ILCs
***
**
B
Nkp44- ILC3
Nkp44+ ILC3
C
SqCC
ADC
CD3
C-Kit
RORγt
D
Number of ILC3 per 10 HPF
*
SqCC
ADC

Figure 10. ILC3 was higher in SqCCs than ADCs in TME

(**A**) Among live lymphocytes, the percentages of total ILCs, ILC1, ILC2, and ILC3 in SqCCs and ADCs of prospective cohort were compared to matched non-tumor lung tissues. (**B**) The percentages of $Npk44^{+}$ and $Npk44^{-}$ ILC3 in SqCCs and ADCs of prospective cohort were compared to matched non-tumor lung tissues. (**C**) Image of the immunofluorescence microscopic examination of ILC3. A circle indicates $CD3^{-}CD117^{+}ROR\gamma t^{+}$ ILC3 in freshly obtained tumor tissues. Scale bars, 50 μm. (**D**) The number of $CD3^{-}CD117^{+}ROR\gamma t^{+}$ ILC3 per 10 high-power fields of each case was measured using immunofluorescence in SqCCs and ADCs of prospective cohort.

3.4 SqCCs exhibit an inverse correlation between ILC1 and ILC3 compared to ADCs

Before, I found that SqCCs exhibited a reduction in the percentage of ILC1 but an increase ILC3 compared to NTLT in all cases of prospective cohort. Regarding the individual subsets of ILCs, increase number of ILC3 population was also observed in the matched cases of SqCCs and NTLT among all cases (**Figure 11A**). By contrast, the percentages of ILC1 and ILC3 were similar in ADCs and NTLT (**Figure 10A**). Furthermore, an inverse correlation between ILC1 and ILC3 was detected in SqCCs with statistical significance but not in ADCs (**Figure 11B**), which correlated with the expression level of the *IL17* transcript in $CD45^+$ immune cells (**Figure 11C**). In study of ILCs in Crohn's disease, DC promoted the conversion between ILC1 and ILC3. So I further analyzed the correlation between ILCs and other immune subsets. The percentages of ILC1 and ILC3 were not related with those of other immune cell subsets including $CD1c^+$ DCs and $CD141^+$ DCs in NSCLCs (**Figure 12A and 12B**). Collectively, these findings indicate that high numbers of ILC3, but low numbers of ILC1, are located in the TME of SqCCs compared to NTLT, which indicates an inverse correlation between these two subsets in SqCCs but not ADCs.

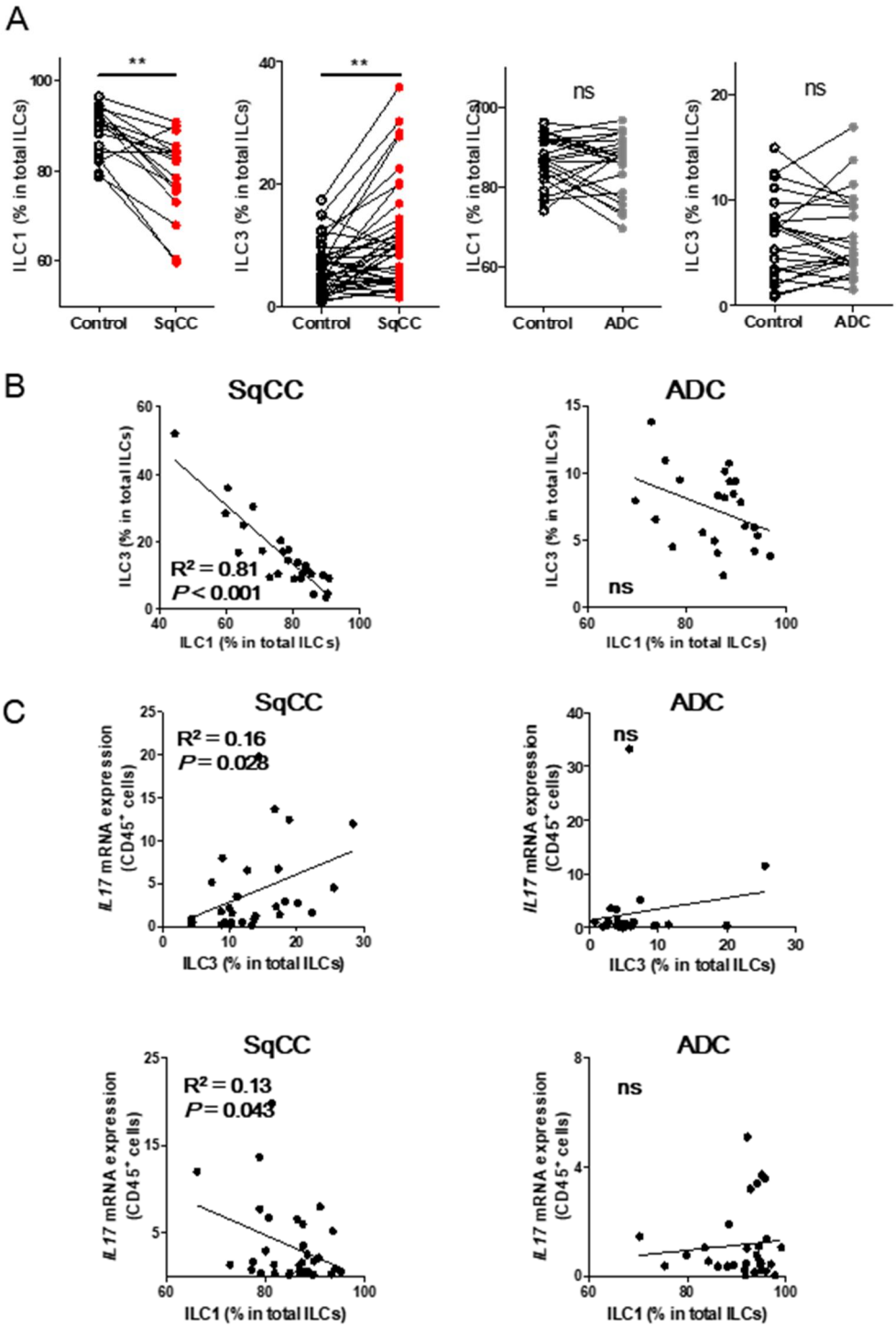
A
**
ILC1 (% in total ILCs)
Control
SqCC
**
ILC3 (% in total ILCs)
Control
SqCC
ns
ILC1 (% in total ILCs)
Control
ADC
ns
ILC3 (% in total ILCs)
Control
ADC
B
SqCC
ILC3 (% in total ILCs)
R² = 0.81
P < 0.001
ILC1 (% in total ILCs)
ADC
ILC3 (% in total ILCs)
ns
ILC1 (% in total ILCs)
C
SqCC
IL17 mRNA expression (CD45⁺ cells)
R² = 0.16
P = 0.028
ILC3 (% in total ILCs)
ADC
IL17 mRNA expression (CD45⁺ cells)
ns
ILC3 (% in total ILCs)
SqCC
IL17 mRNA expression (CD45⁺ cells)
R² = 0.13
P = 0.043
ILC1 (% in total ILCs)
ADC
IL17 mRNA expression (CD45⁺ cells)
ns
ILC1 (% in total ILCs)

Figure 11. Inverse correlation between ILC1 and ILC3 in pulmonary SqCC.

(**A**) Comparative analyses of the percentages of ILC1 and ILC3 among ILCs in SqCCs and ADCs compared to matched NTLT freshly obtained from patients. (**B**) Correlations between the percentages of ILC1 and ILC3 among total ILCs in SqCCs and ADCs were analyzed. (**C**) Correlations between the percentages of ILC3 among total ILCs and the expression levels of the *IL17* transcript of $CD45^{+}EpCAM^{-}$ immune cells freshly isolated from SqCCs and ADCs.

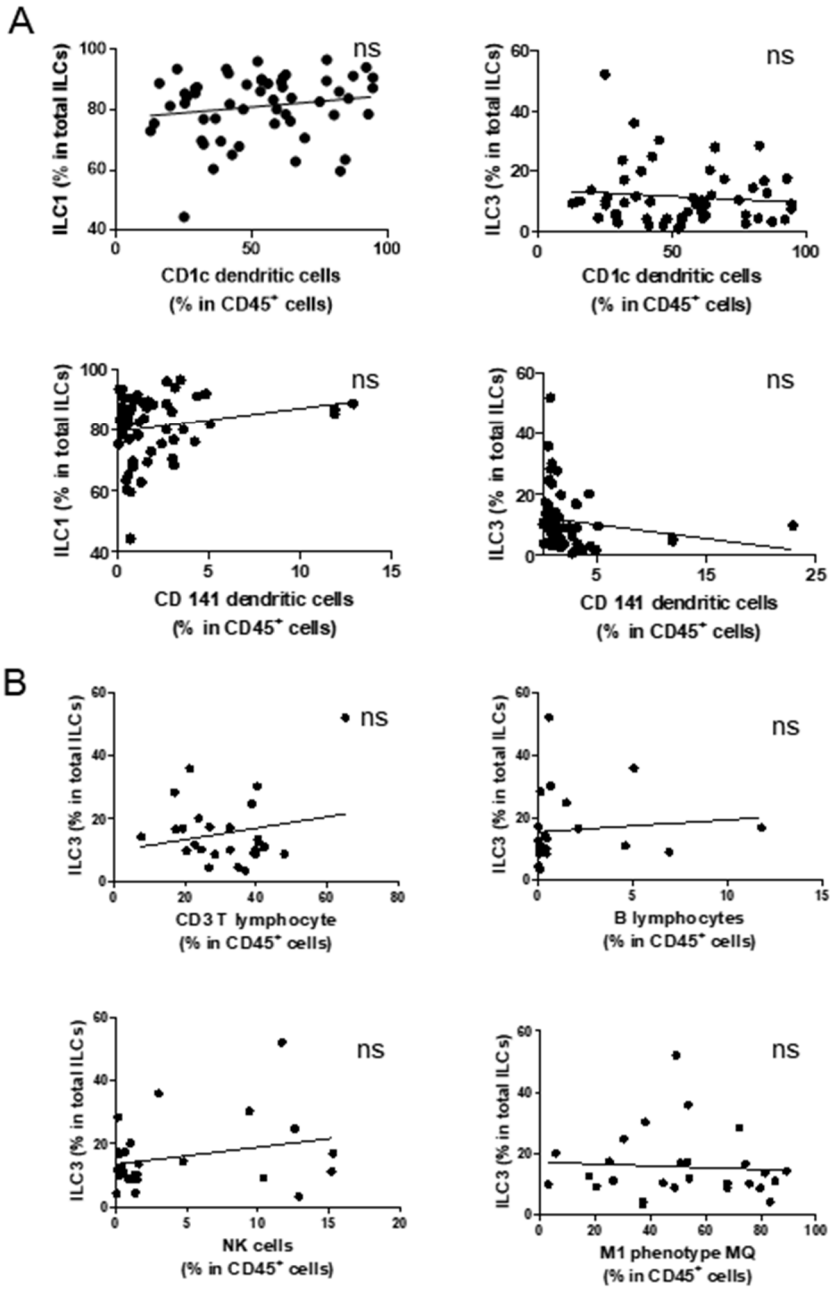
A
ILC1 (% in total ILCs)
ns
CD1c dendritic cells
(% in CD45+ cells)
ILC3 (% in total ILCs)
ns
CD1c dendritic cells
(% in CD45+ cells)
ILC1 (% in total ILCs)
ns
CD 141 dendritic cells
(% in CD45+ cells)
ILC3 (% in total ILCs)
ns
CD 141 dendritic cells
(% in CD45+ cells)
B
ILC3 (% in total ILCs)
ns
CD3 T lymphocyte
(% in CD45+ cells)
ILC3 (% in total ILCs)
ns
B lymphocytes
(% in CD45+ cells)
ILC3 (% in total ILCs)
ns
NK cells
(% in CD45+ cells)
ILC3 (% in total ILCs)
ns
M1 phenotype MQ
(% in CD45+ cells)

Figure 12. The subsets of ILCs don't correlated with other immune subsets in TME.

(**A**) Correlation analyses between the percentage of ILC1 or ILC3 among total ILCs and those of $CD1c^+$ and $CD141^+$ dendritic cells among $CD45^+$ immune cells. (**B**) Association between ILC and various kinds of immune subsets, including CD3 T lymphocytes, B lymphocytes, NK cells and M1 phenotype macrophages. Data are presented as the mean ± SEM. *p <0.05, **p <0.01, ***p <0.001. (NS, non-significant)

3.5 Conversion from ILC1 into ILC3 is promoted by IL-23-producing SqCCs, rather than immune cells, in the TME

IL-23 and IL-1β induce the conversion of ILC1 into ILC3 (27, 32). Thus, to investigate the mechanism by which SqCCs lead to high numbers of ILC3 but low numbers of ILC1 in the TME, I measured the expression levels of these cytokines in $CD45^+$ immune and $CD45^-$ $EpCAM^+$ tumor cells freshly obtained from NSCLCs and analyzed the correlations between these cells and the percentages of ILC1 and ILC3 subsets. In NSCLCs, the expression level of *IL23p19* transcript in $CD45^-$ $EpCAM^+$ tumor cells, but not $CD45^+$ immune cells, was positively correlated with the percentage of ILC3 but inversely associated with that of ILC1 (**Figure 13A**). By contrast, none of the *IL1β*, *IL12*, or *IL18* transcript levels in tumor and immune cells were significantly associated with ILC subsets in NSCLCs (**Figure 13A and 13B**). Moreover, flow cytometric analyses revealed that the percentage of IL-23^+ tumor cells was positively correlated with that of ILC3 in NSCLCs, whereas that in IL-23^+ immune cells was not (**Figure 13C**). These findings suggest that IL-23-producing NSCLCs are involved in the plasticity of ILC subsets by converting ILC1 into ILC3 in the TME. Among NSCLCs, SqCCs express higher transcript levels of *IL23* in $CD45^-$ $EpCAM^+$ tumor cells than ADCs, whereas $CD45^+$ immune cells similarly express these cytokines in the two histological types of NSCLCs (**Figure 13D**), consistent with data from TCGA (**Figure 13E**). Flow cytometric analyses demonstrated higher percentages of

IL-23-expressing $CD45^{-}EpCAM^{+}$ tumor cells and their cytosolic expression of IL-23 in SqCCs than ADCs, whereas the percentages of IL-23-positive $CD45^{+}$ immune cells were similar in the two types of NSCLCs and were not associated with the percentage of ILC3 (**Figure 13F and 13G**). These findings suggest that IL-23-producing SqCCs, rather than immune cells, promote the conversion of ILC1 into ILC3 in the TME.

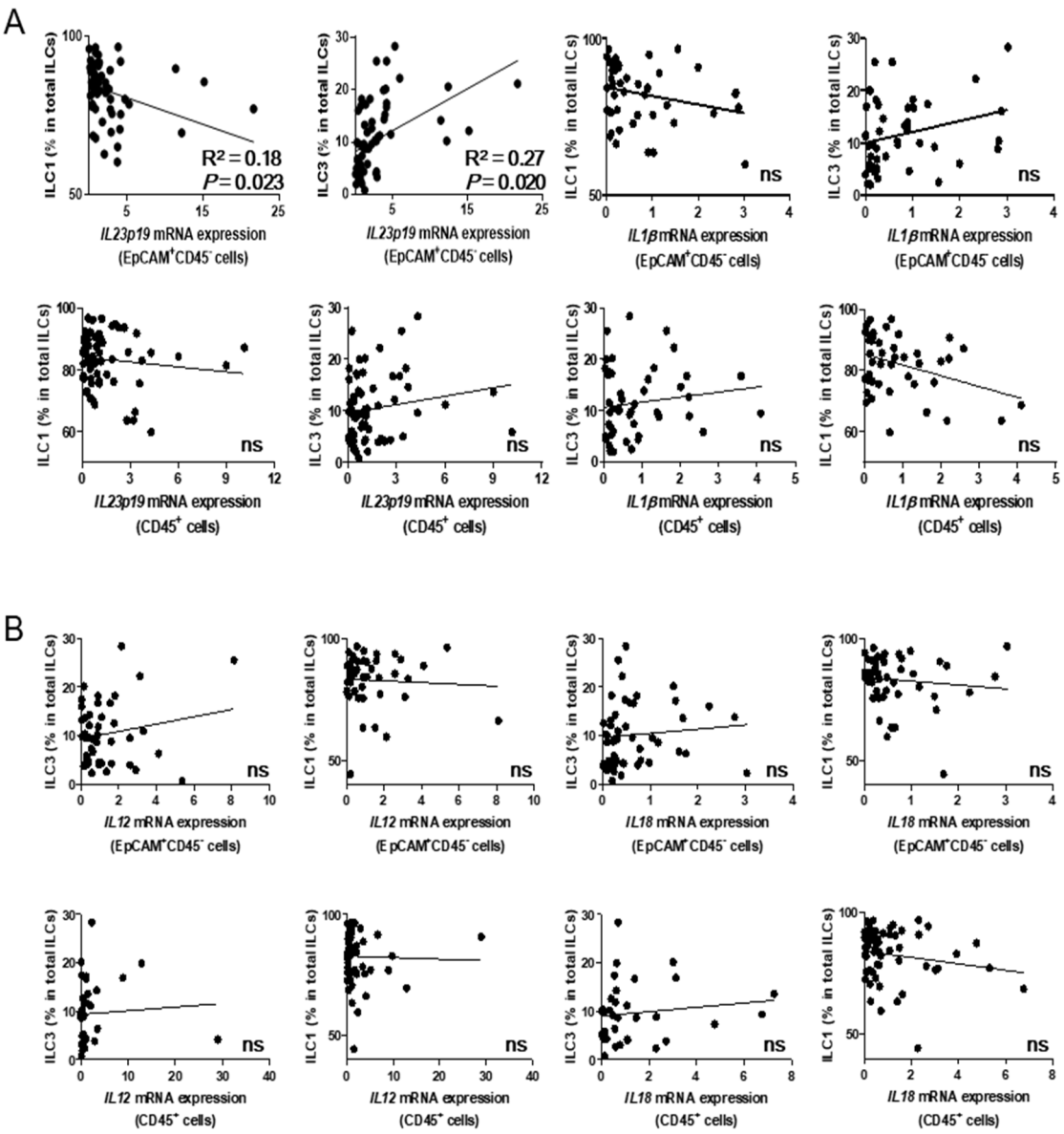
A
ILC1 (% in total ILCs)
R² = 0.18
P = 0.023
IL23p19 mRNA expression
(EpCAM+CD45- cells)
ILC3 (% in total ILCs)
R² = 0.27
P = 0.020
IL23p19 mRNA expression
(EpCAM+CD45- cells)
ILC1 (% in total ILCs)
ns
IL1β mRNA expression
(EpCAM+CD45- cells)
ILC3 (% in total ILCs)
ns
IL1β mRNA expression
(EpCAM+CD45- cells)
ILC1 (% in total ILCs)
ns
IL23p19 mRNA expression
(CD45+ cells)
ILC3 (% in total ILCs)
ns
IL23p19 mRNA expression
(CD45+ cells)
ILC3 (% in total ILCs)
ns
IL1β mRNA expression
(CD45+ cells)
ILC1 (% in total ILCs)
ns
IL1β mRNA expression
(CD45+ cells)
B
ILC3 (% in total ILCs)
ns
IL12 mRNA expression
(EpCAM+CD45- cells)
ILC1 (% in total ILCs)
ns
IL12 mRNA expression
(EpCAM+CD45- cells)
ILC3 (% in total ILCs)
ns
IL18 mRNA expression
(EpCAM+CD45- cells)
ILC1 (% in total ILCs)
ns
IL18 mRNA expression
(EpCAM+CD45- cells)
ILC3 (% in total ILCs)
ns
IL12 mRNA expression
(CD45+ cells)
ILC1 (% in total ILCs)
ns
IL12 mRNA expression
(CD45+ cells)
ILC3 (% in total ILCs)
ns
IL18 mRNA expression
(CD45+ cells)
ILC1 (% in total ILCs)
ns
IL18 mRNA expression
(CD45+ cells)

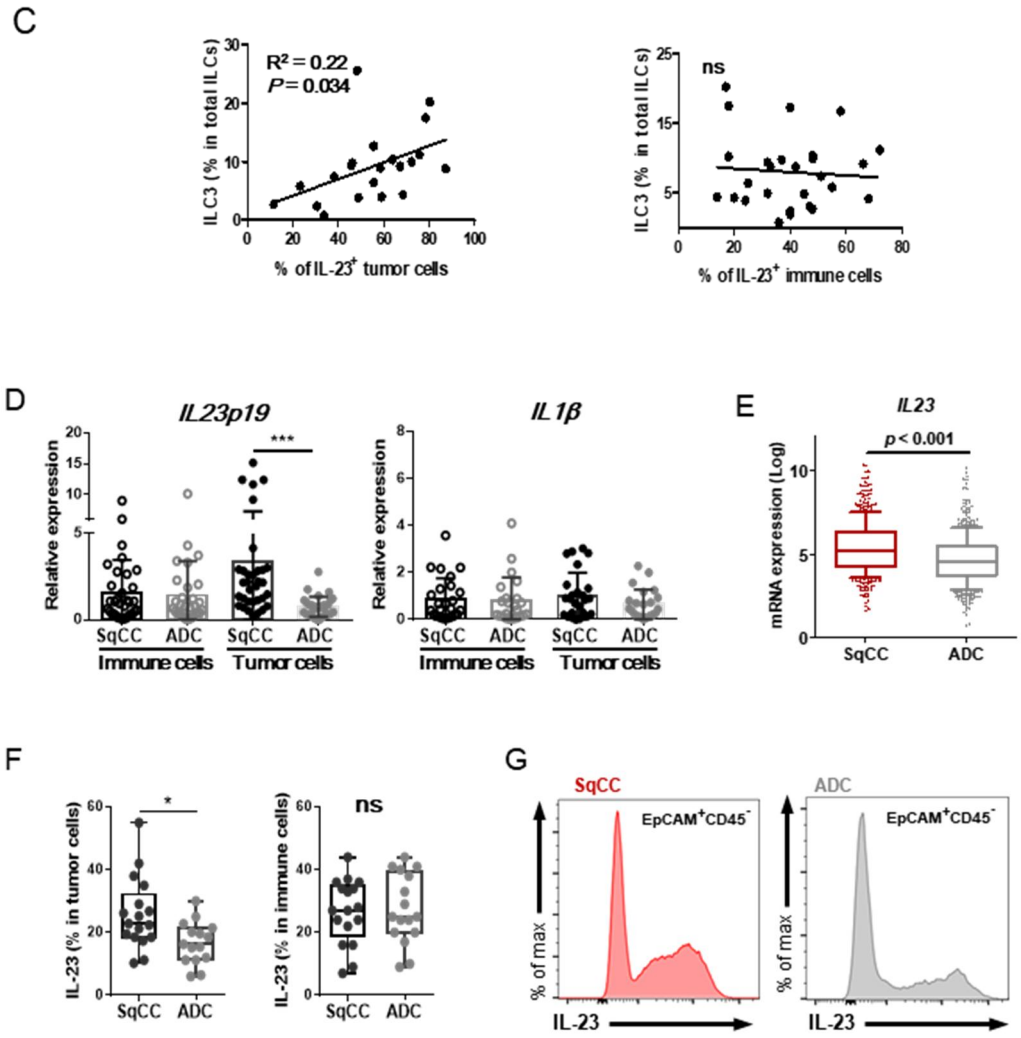
C
R² = 0.22
P = 0.034
ILC3 (% in total ILCs)
% of IL-23+ tumor cells
ns
ILC3 (% in total ILCs)
% of IL-23+ immune cells
D
IL23p19
Relative expression
***
SqCC
ADC
SqCC
ADC
Immune cells
Tumor cells
IL1β
Relative expression
SqCC
ADC
SqCC
ADC
Immune cells
Tumor cells
E
IL23
p < 0.001
mRNA expression (Log)
SqCC
ADC
F
IL-23 (% in tumor cells)
*
SqCC
ADC
IL-23 (% in immune cells)
ns
SqCC
ADC
G
SqCC
EpCAM+CD45-
% of max
IL-23
ADC
EpCAM+CD45-
% of max
IL-23

Figure 13. The percentages of ILC3 is associated with the expression of IL-23 in tumor cells, rather than CD45$^+$ immune cells.

(**A**) Correlations between the levels of *IL23p19* and *IL1B* in EpCAM$^+$CD45$^-$ tumor cells or CD45$^+$ immune cells freshly isolated from NSCLCs and the percentages of ILC1 or ILC3 in the TME. (**B**) Correlations between the levels of *IL12* and *IL18* in EpCAM$^+$CD45$^-$ tumor cells or CD45$^+$ immune cells of NSCLCs and the percentages of ILC1 or ILC3 in the TME. (**C**) Correlations between the percentages of IL-23-expressing cells among EpCAM$^+$CD45$^-$ tumor cells or CD45$^+$ immune cells in NSCLCs and the percentages of ILC3 among total ILCs in the TME. (**D**) Expression levels of the *IL23p19* and *IL1B* transcripts in EpCAM$^+$CD45$^-$ tumor cells or CD45$^+$ immune cells from SqCCs and ADCs. (**E**) Analysis for *IL23* transcription levels in two types of NSCLCs using TCGA data. (**F**) Percentages of IL-23$^+$ tumor cells or IL-23$^+$ immune cells of SqCCs and ADCs. **(G)** Flow cytometric analyses of the cytosolic expression of IL-23-expressing cells among EpCAM$^+$CD45$^-$ tumor cells in SqCCs and ADCs. Data are presented as the mean ± SEM. *p <0.05, **p <0.01, ***p <0.001.

3.6 SqCCs rather than ADCs drive the conversion from ILC1 into ILC3 subsets by producing IL-23

To support my suggestion, I cultured total ILCs or ILC1 sorted from NTLT in the presence of IL-2 and IL-23. Recombinant IL-2 + IL-23 or IL-23 increased the percentage of ILC3 after co-culture with total ILCs or ILC1 for 5 days, which was decreased by treatment with an anti-IL-23 neutralizing monoclonal antibody (mAb), which indicates that IL-23 promotes the conversion from ILC1 into ILC3 in lung tissue (**Figure 14A and 14B**). ILC subsets were defined according to expression pattern of transcription factors (RORγt and GATA3) as well as cell surface markers (c-kit and IL-7Rα). The percentage of ILC3 was higher in co-culture of total ILCs from ADCs and $CD45^-EpCAM^+$ tumor cells of SqCC, but not those from ADCs with IL-23 dependency (**Figure 15A and 15B**). Co-culture of ILCs from SqCC and $CD45^-EpCAM^+$ tumor cells from SqCC or ADC did not alter the ILC3 population (**Figure 15C and 15D**). Furthermore, co-culture with sorted ILC1 from NTLT or ADC tumor cells, and $CD45^-EpCAM^+$ tumor cells of SqCC increased the percentage of ILC3 but reduced that of ILC1, which was inhibited by adding the neutralizing IL-23 mAb (**Figure 15E and 15F**). By contrast, $CD45^-EpCAM^+$ tumor cells of ADCs did not alter the percentages of ILC1 and ILC3 during co-culture with sorted ILC1 (**Figure 15E and 15F**). These findings indicate that SqCCs rather than ADCs drive the conversion from ILC1 into ILC3 subsets by producing IL-23 in NTLT and TME.

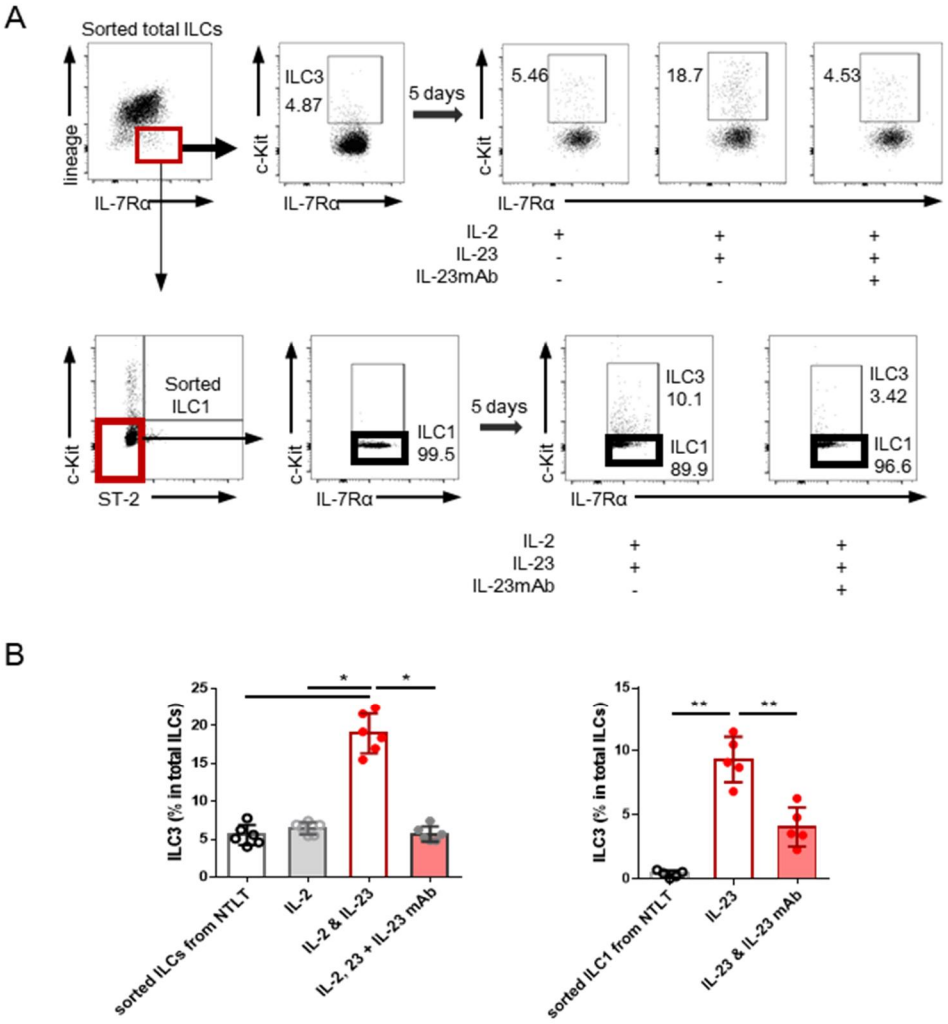
A
Sorted total ILCs
lineage
IL-7Rα
c-Kit
ILC3
4.87
5 days
5.46
18.7
4.53
IL-2
IL-23
IL-23mAb
Sorted
ILC1
ST-2
ILC1
99.5
ILC3
10.1
ILC1
89.9
ILC3
3.42
ILC1
96.6
B
ILC3 (% in total ILCs)
sorted ILCs from NTLT
IL-2
IL-2 & IL-23
IL-2, 23 + IL-23 mAb
sorted ILC1 from NTLT
IL-23
IL-23 & IL-23 mAb

Figure 14. Conversion from ILC1 into ILC3 is promoted in an IL-23-dependent manner.

The ILC subsets were defined using suface markers including c-kit and IL-7Rα. (**A**) Representative gating figure of **t**he percentage of ILC3 was measured after total ILCs or ILC1 sorted from non-tumor lung tissues (NTLT) were co-cultured with recombinant IL-2 or IL-2 + IL-23 in the presence or absence of anti-IL-23-neutralizing antibody for 5 days. (**B**) Bar graph of the percentages of ILC3. The results were pooled from at least five independent experiments, analyzed, and are presented in graphs. Diagrams for flow cytometric analyses are a representative result of these experiments. Data are presented as the mean ± SEM. *p <0.05, **p <0.01, ***p <0.001.

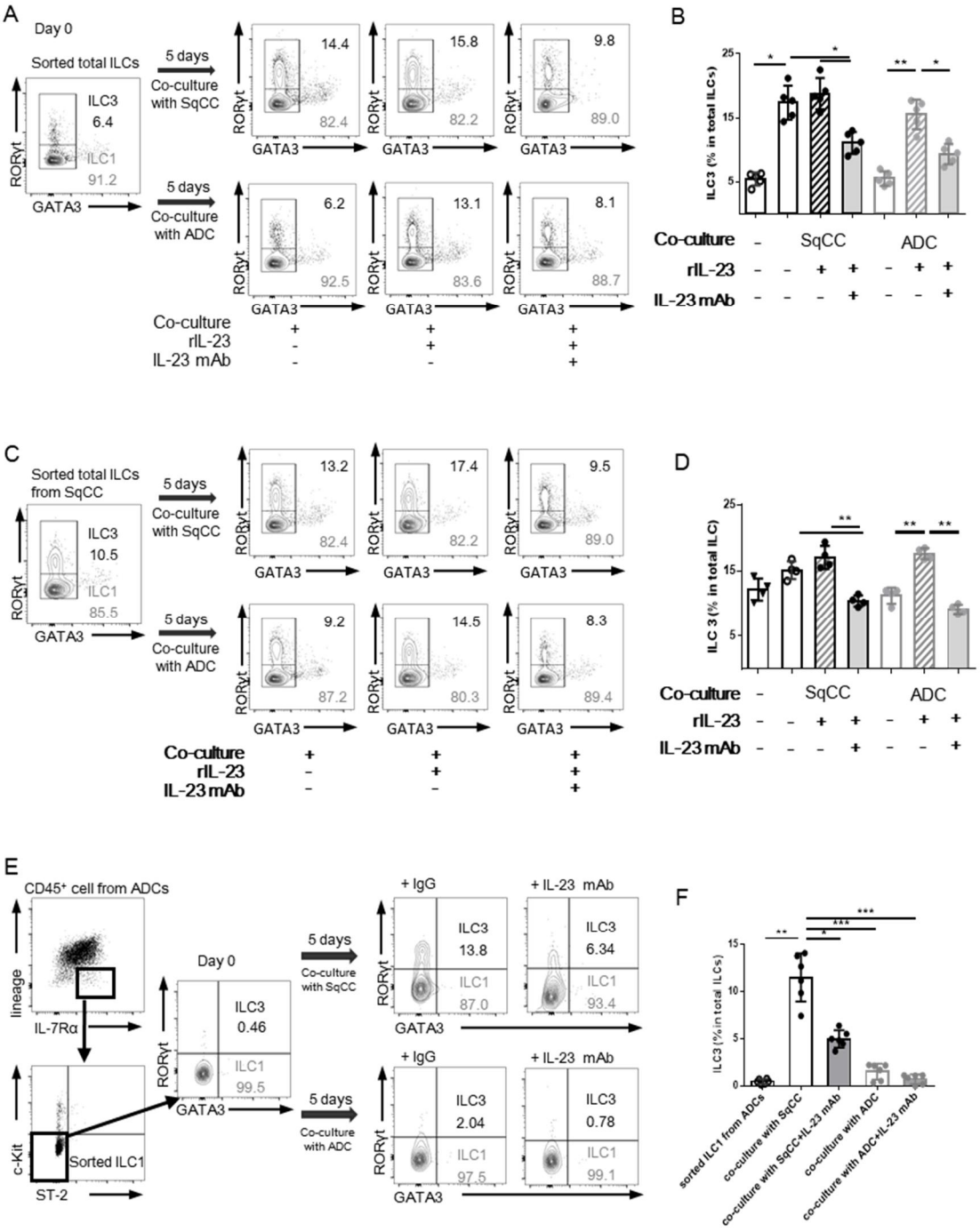
A
Day 0
Sorted total ILCs
ILC3
6.4
ILC1
91.2
RORγt
GATA3
5 days
Co-culture with SqCC
14.4
82.4
15.8
82.2
9.8
89.0
5 days
Co-culture with ADC
6.2
92.5
13.1
83.6
8.1
88.7
Co-culture
rIL-23
IL-23 mAb
B
ILC3 (% in total ILCs)
Co-culture
SqCC
ADC
rIL-23
IL-23 mAb
C
Sorted total ILCs from SqCC
ILC3
10.5
ILC1
85.5
5 days
Co-culture with SqCC
13.2
82.4
17.4
82.2
9.5
89.0
5 days
Co-culture with ADC
9.2
87.2
14.5
80.3
8.3
89.4
Co-culture
rIL-23
IL-23 mAb
D
ILC 3 (% in total ILC)
Co-culture
SqCC
ADC
rIL-23
IL-23 mAb
E
CD45+ cell from ADCs
lineage
IL-7Rα
c-Kit
ST-2
Sorted ILC1
Day 0
ILC3
0.46
ILC1
99.5
5 days
Co-culture with SqCC
5 days
Co-culture with ADC
+ IgG
+ IL-23 mAb
ILC3
13.8
ILC1
87.0
ILC3
6.34
ILC1
93.4
ILC3
2.04
ILC1
97.5
ILC3
0.78
ILC1
99.1
F
ILC3 (% in total ILCs)
sorted ILC1 from ADCs
co-culture with SqCC
co-culture with SqCC+IL-23 mAb
co-culture with ADC
co-culture with ADC+IL-23 mAb

Figure 15. Conversion from ILC1 into ILC3 is promoted by SqCCs, not ADCs, in an IL-23-dependent manner.

The ILC subsets were defined using intracellular expression of transcription facotrs including RORγt and GATA3. (**A** and **B**) The percentages of ILC3 among total ILCs were measured after ILCs sorted from ADCs were co-cultured with tumor cells from SqCCs or ADCs in the presence or absence of anti-IL-23 antibody for 5 days. (**C** and **D**) The percentages of ILC3 among total ILCs were measured after ILCs sorted from SqCCs were co-cultured with tumor cells from SqCCs or ADCs for 5 days. (**E** and **F**) The percentages of ILC3 among total ILCs were measured after ILC1 sorted from ADCs was co-cultured with tumor cells from SqCCs or ADCs for 5 days. The results were pooled from at least five independent experiments, analyzed, and are presented in graphs. Diagrams for flow cytometric analyses are a representative result of these experiments. Data are presented as the mean ± SEM. *p <0.05, **p <0.01, ***p <0.001.

3.7 IL-23-producing SqCCs promote tumor growth by inducing ILC3-mediated IL-17 production in *in vitro*

To explore IL-23-ILC3-IL-17 axis in tumor proliferation *in vitro*, I cultured ILC1 from the IL-23^{low} ADC + IL-23^{high} SqCC cell line (SK-MES1, H1703, or HCC15) or tumor cells freshly isolated from SqCCs in the presence of the anti-IL-23, anti-IL-17, or anti-IL-22 mAb (**Figure 16A**). The percentages of ILC3 among total ILCs and amounts IL-17 in culture supernatants were increased after co-culture of ILC1 and the SqCC cell line, whereas those of ILC1 were decreased. These alterations were inhibited by adding the anti-IL-23 antibody, but not by the anti-IL-22, anti-IL-17 or anti-IL-1β-neutralizing antibody (**Figure 16A - C**). The expression levels of proliferation markers in tumor cells were also increased during co-culture of ILC1 and the SqCC cell line, which was inhibited by adding the anti-IL-23 or anti-IL-17 antibody (**Figure 16D**). The co-culture experiments using tumor cells from cancer patients showed increased expression of proliferation-related markers and Ki-67 index during co-culture of ILC1 and SqCC tumor cells (**Figure 17A and 17B**). Moreover, IL-17 production was detected in ILC3, but not ILC2 (**Figure 17C**). The percentage of IL-22^{+} ILCs was similar in SqCCs and ADCs, and the expression level of the *IL22* transcript was not significantly associated with percentage of ILC3 in NSCLCs (**Figure 17D and 17E**). These findings indicate that IL-23-producing SqCCs promote tumor growth by inducing ILC3-mediated IL-17 production, although they increase the production of IL-17 and IL-22.

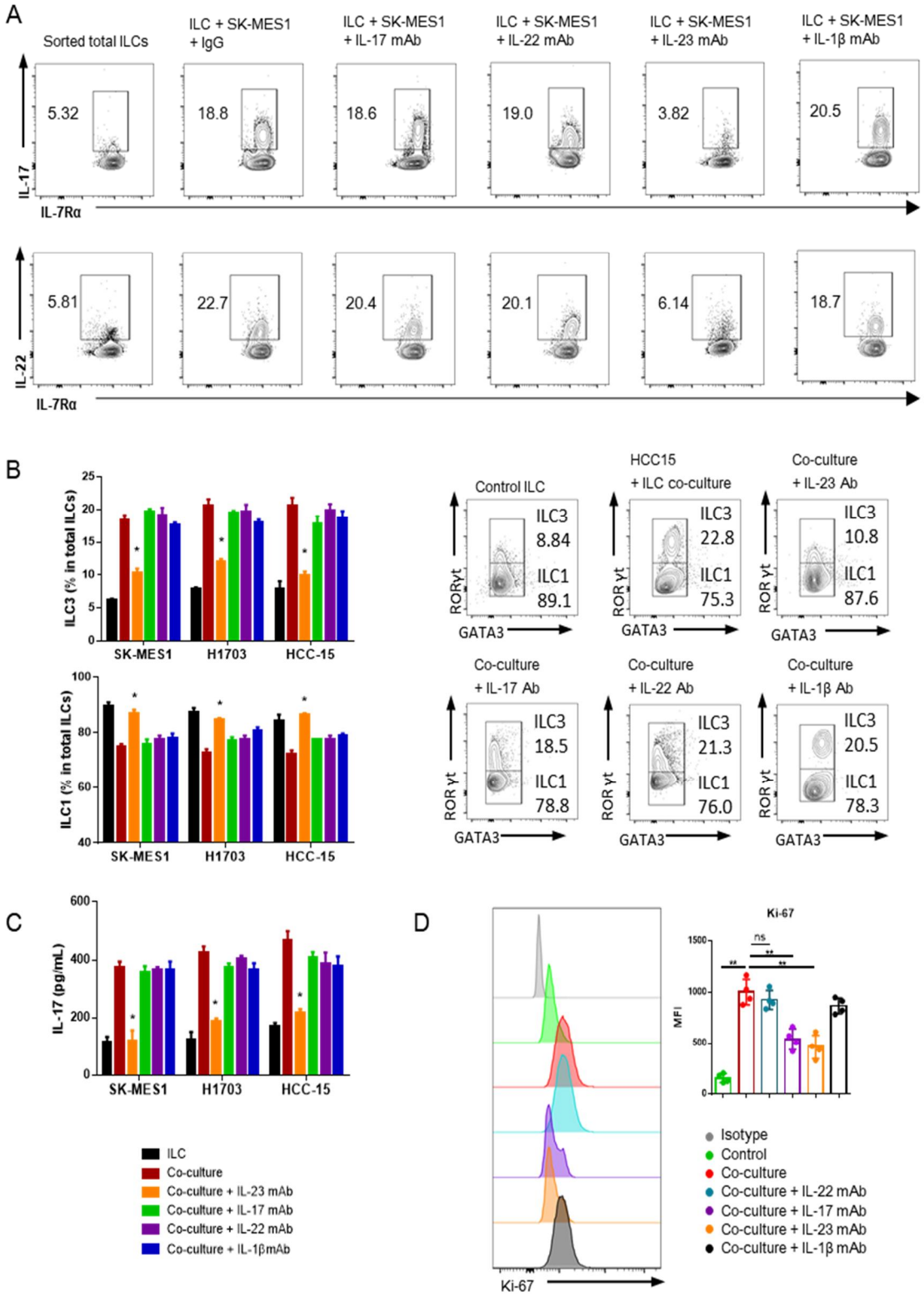
A
Sorted total ILCs
ILC + SK-MES1 + IgG
ILC + SK-MES1 + IL-17 mAb
ILC + SK-MES1 + IL-22 mAb
ILC + SK-MES1 + IL-23 mAb
ILC + SK-MES1 + IL-1β mAb
5.32
18.8
18.6
19.0
3.82
20.5
IL-17
IL-7Rα
5.81
22.7
20.4
20.1
6.14
18.7
IL-22
IL-7Rα
B
ILC3 (% in total ILCs)
ILC1 (% in total ILCs)
SK-MES1
H1703
HCC-15
Control ILC
HCC15 + ILC co-culture
Co-culture + IL-23 Ab
ILC3 8.84
ILC1 89.1
ILC3 22.8
ILC1 75.3
ILC3 10.8
ILC1 87.6
Co-culture + IL-17 Ab
Co-culture + IL-22 Ab
Co-culture + IL-1β Ab
ILC3 18.5
ILC1 78.8
ILC3 21.3
ILC1 76.0
ILC3 20.5
ILC1 78.3
RORγt
GATA3
C
IL-17 (pg/mL)
SK-MES1
H1703
HCC-15
ILC
Co-culture
Co-culture + IL-23 mAb
Co-culture + IL-17 mAb
Co-culture + IL-22 mAb
Co-culture + IL-1βmAb
D
Ki-67
MFI
ns
Isotype
Control
Co-culture
Co-culture + IL-22 mAb
Co-culture + IL-17 mAb
Co-culture + IL-23 mAb
Co-culture + IL-1β mAb

Figure 16. IL-23-ILC3-IL-17 axis in tumor proliferation *in vitro*

The experiments were perfromed by co-culture ILC1 sorted from ADCs with the SqCC cell lines in the presence or absence of anti-IL-17, anti-IL-22, anti-IL-23, or anti-IL-1β antibody for 5 days. The results were pooled from four independent experiments and analyzed.

(**A**) The cytosolic expression of IL-17 or IL-22 in ILC3 , (**B**) ILC subsets, (**C**) amounts of IL-17 in culture supernatants, (**D**) expression levels of Ki-67 in tumor cells

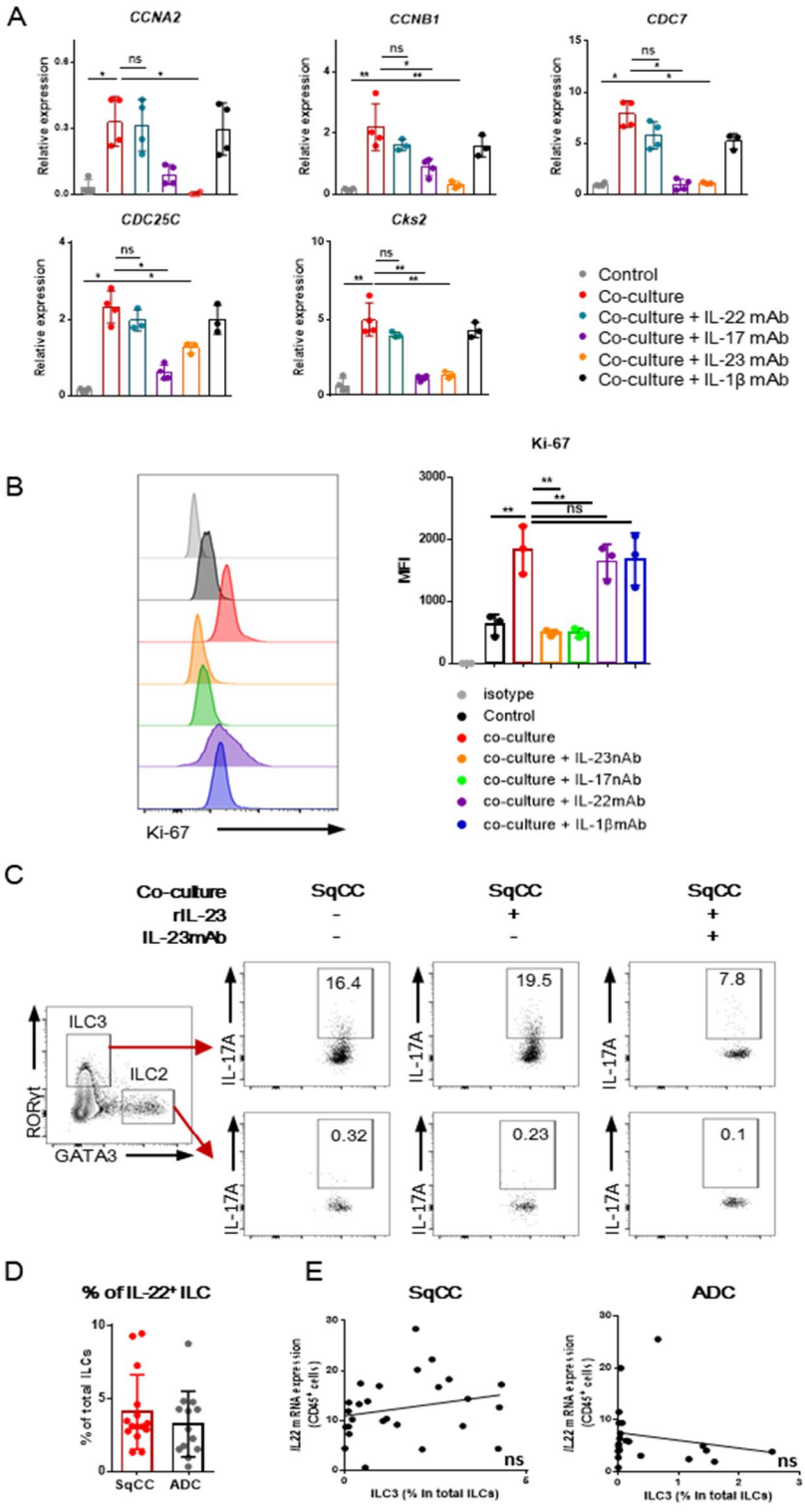
A
CCNA2
CCNB1
CDC7
CDC25C
Cks2
Relative expression
ns
Control
Co-culture
Co-culture + IL-22 mAb
Co-culture + IL-17 mAb
Co-culture + IL-23 mAb
Co-culture + IL-1β mAb
B
Ki-67
MFI
isotype
Control
co-culture
co-culture + IL-23nAb
co-culture + IL-17nAb
co-culture + IL-22mAb
co-culture + IL-1βmAb
C
Co-culture
rIL-23
IL-23mAb
SqCC
ILC3
ILC2
RORγt
GATA3
IL-17A
16.4
19.5
7.8
0.32
0.23
0.1
D
% of IL-22+ ILC
% of total ILCs
SqCC
ADC
E
SqCC
ADC
IL22 mRNA expression (CD45+ cells)
ILC3 (% in total ILCs)
ns

Figure 17. IL-23-ILC3-IL-17 axis in tumor proliferation using cancer cells from patients *in vitro*

The experiments were perfromed by co-culture ILC1 sorted from ADCs with tumor cells freshly isolated from SqCCs in the presence or absence of anti-IL-17, anti-IL-22, anti-IL-23, or anti-IL-1β antibody for 5 days. The results were pooled from four independent experiments and analyzed.

(**A**) Expression level of proliferation-related molecules and (**B**) expression levels of Ki-67 in tumor cells were analyzed using flow cytometry. Data are representative of at least three independent experiments. (**C**) Cytosolic IL-17 in ILC2 and ILC3 was analyzed using flow cytometry (**D**) The percentages of IL-22^{+} ILCs among total ILCs were analyzed in SqCCs and ADCs. (**E**) Correlations between the expression level of the *IL22* transcript and the percentage of ILC3 among total ILCs in SqCCs and ADCs.

3.8 IL-23-producing SqCCs promote tumor growth by inducing ILC3-mediated IL-17 production in *in vivo*

To confirm this *in vivo*, I injected WT mice subcutaneously with IL-23-overexpressing mouse SqCC cell line (KLN-205 transduced by IL-23-overexpressing lentivirus) or control cells (KLN 205 with empty vector). IL-23-overexpressing KLN-205 cells increased tumor sizes more than control and WT KLN-205 cells, which was abolished by injecting with anti-IL-23 blocking antibody (**Figure 18A and 18B**). Moreover, the percentages of ILC3 and IL-17-expressing ILCs were higher in tumors from mice injected IL-23-expressing KLN-205 cells than control or WT KLN-205 cells, whereas those of ILC1 were lower. This inverse correlation between ILC3 and ILC1 and enhancement of IL-17-expressing ILCs in tumors were also inhibited by anti-IL-23 antibody injection (**Figure 18C - G**). However, the percentages of ILC2 were similar in the tumors of all groups (**Figure 18E**). These findings indicate that IL-23 produced by SqCC cells promotes tumor growth by increasing IL-17-producing ILC3 in TME.

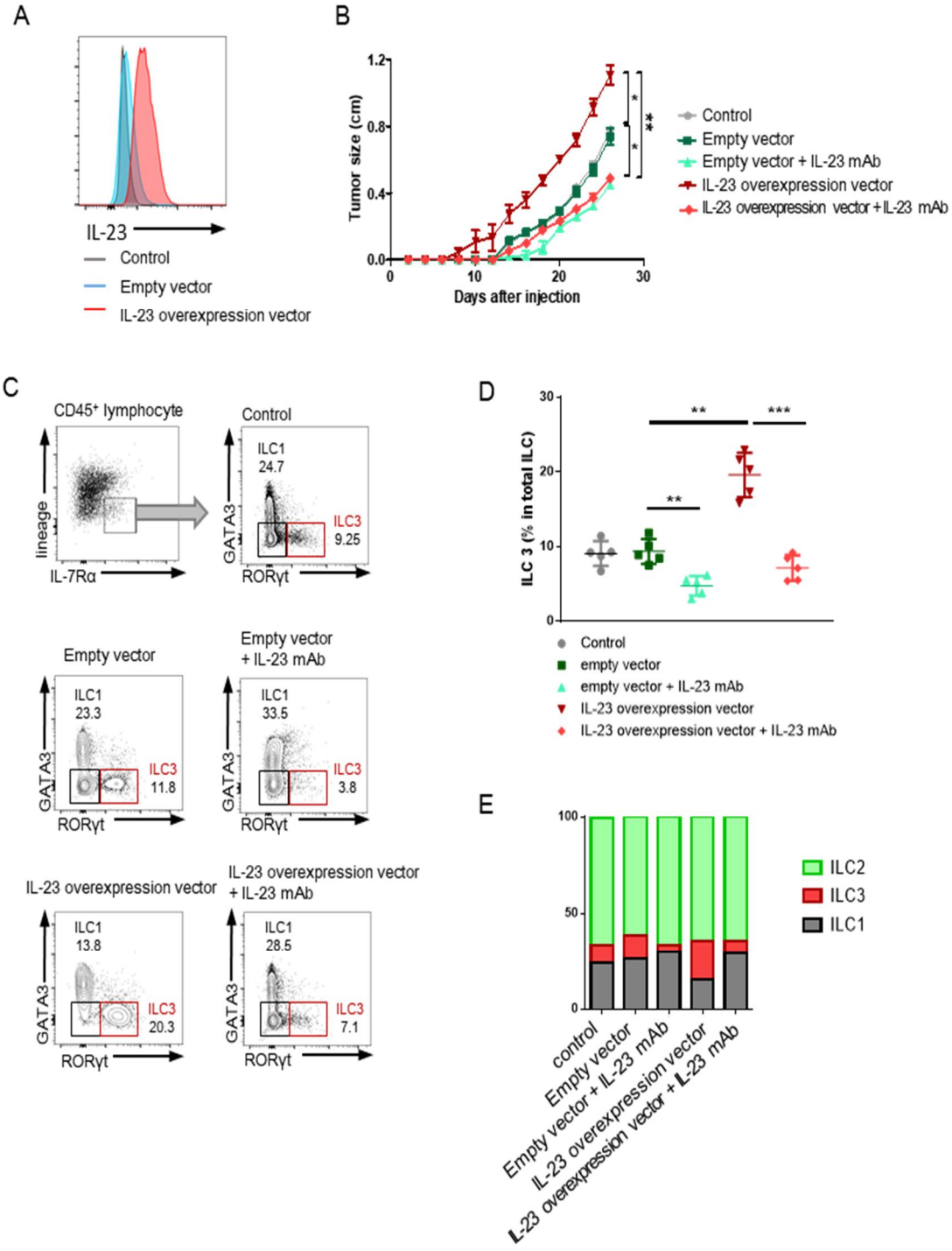
A
IL-23
Control
Empty vector
IL-23 overexpression vector
B
Tumor size (cm)
Days after injection
Control
Empty vector
Empty vector + IL-23 mAb
IL-23 overexpression vector
IL-23 overexpression vector + IL-23 mAb
C
CD45+ lymphocyte
lineage
IL-7Rα
Control
ILC1 24.7
ILC3 9.25
GATA3
RORγt
Empty vector
ILC1 23.3
ILC3 11.8
Empty vector + IL-23 mAb
ILC1 33.5
ILC3 3.8
IL-23 overexpression vector
ILC1 13.8
ILC3 20.3
IL-23 overexpression vector + IL-23 mAb
ILC1 28.5
ILC3 7.1
D
ILC 3 (% in total ILC)
Control
empty vector
empty vector + IL-23 mAb
IL-23 overexpression vector
IL-23 overexpression vector + IL-23 mAb
E
ILC2
ILC3
ILC1
control
Empty vector
Empty vector + IL-23 mAb
IL-23 overexpression vector
IL-23 overexpression vector + IL-23 mAb

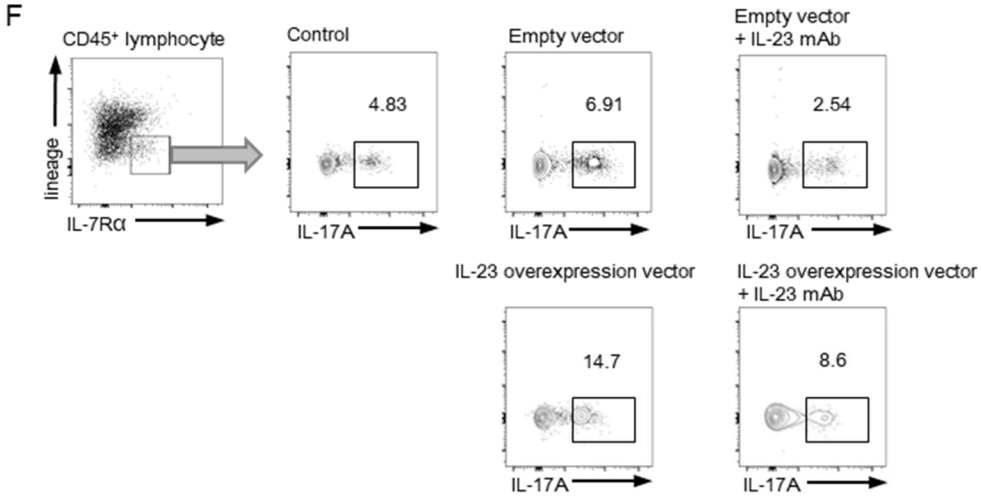
F
CD45+ lymphocyte
lineage
IL-7Rα
Control
4.83
IL-17A
Empty vector
6.91
IL-17A
Empty vector
+ IL-23 mAb
2.54
IL-17A
IL-23 overexpression vector
14.7
IL-17A
IL-23 overexpression vector
+ IL-23 mAb
8.6
IL-17A

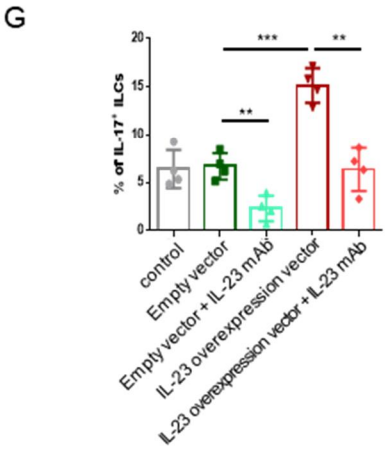
G
% of IL-17+ ILCs
20
15
10
5
0
***
**
**
control
Empty vector
Empty vector + IL-23 mAb
IL-23 overexpression vector
IL-23 overexpression vector + IL-23 mAb

Figure 18. ILC3 promotes the proliferation of SqCCs in an IL-17-dependent manner *in vivo*.

(**A**) The cytosolic expression of IL-23 in a mouse SqCC line (KLN-205) cells transduced by IL-23-expressing lentivirus or empty vector, and control untrasduced KLN-205 cells. (**B - G**) Measurement of tumor sizes (**B**), percentages of ILC subsets (**C - E**) and IL-17$^+$ ILCs (**F** and **G**) among total ILCs in WT mice injected KLN-205 cells transduced by IL-23-expressing lentivirus or empty vector, and control untrasduced KNL-205 cells in the presence or absence of anti-IL-23 antibody administration. Data are presented as the mean ± SEM. *p <0.05, **p <0.01, ***p <0.001. n = 4 in each group

3.9 ILC3 contributes to the poor prognosis of patients with SqCC

Before, I insisted that IL-23 produced by SqCC cells promotes tumor growth by increasing IL-17-producing ILC3 in TME. To address this in patients with NSCLC, I analyzed the survival of patients with SqCC or ADC by estimating the numbers of $CD3^-CD20^-ROR\gamma t^+$ ILC3 and the expression of IL-23 in tumor cells using immunohistochemistry (**Figure 19A - E**). The expression of ILC3 was estimated by loss of brown expression of CD3 or CD20, positive blue nuclear expression of RORγt. SqCCs exhibited higher numbers of IL-23-expessing tumor cells and $CD3^-CD20^-ROR\gamma t^+$ILC3 in the TME than ADCs (**Figure 19C and 19D**). The numbers of $CD3^-CD20^-ROR\gamma t^+$ILC3 were higher in IL-23^+ tumor cells than IL-23^- cells in NSCLCs (**Figure 19E**). Moreover, the numbers of $CD3^-CD20^-ROR\gamma t^+$ILC3 and the expression of IL-23 in tumor cells were significantly associated with short progression free survival of patients with SqCC, but not ADC (**Figure 19F**). These findings indicate that the IL-23-ILC3-IL-17 axis contributes to a poor prognosis of patients with SqCCs among NSCLCs.

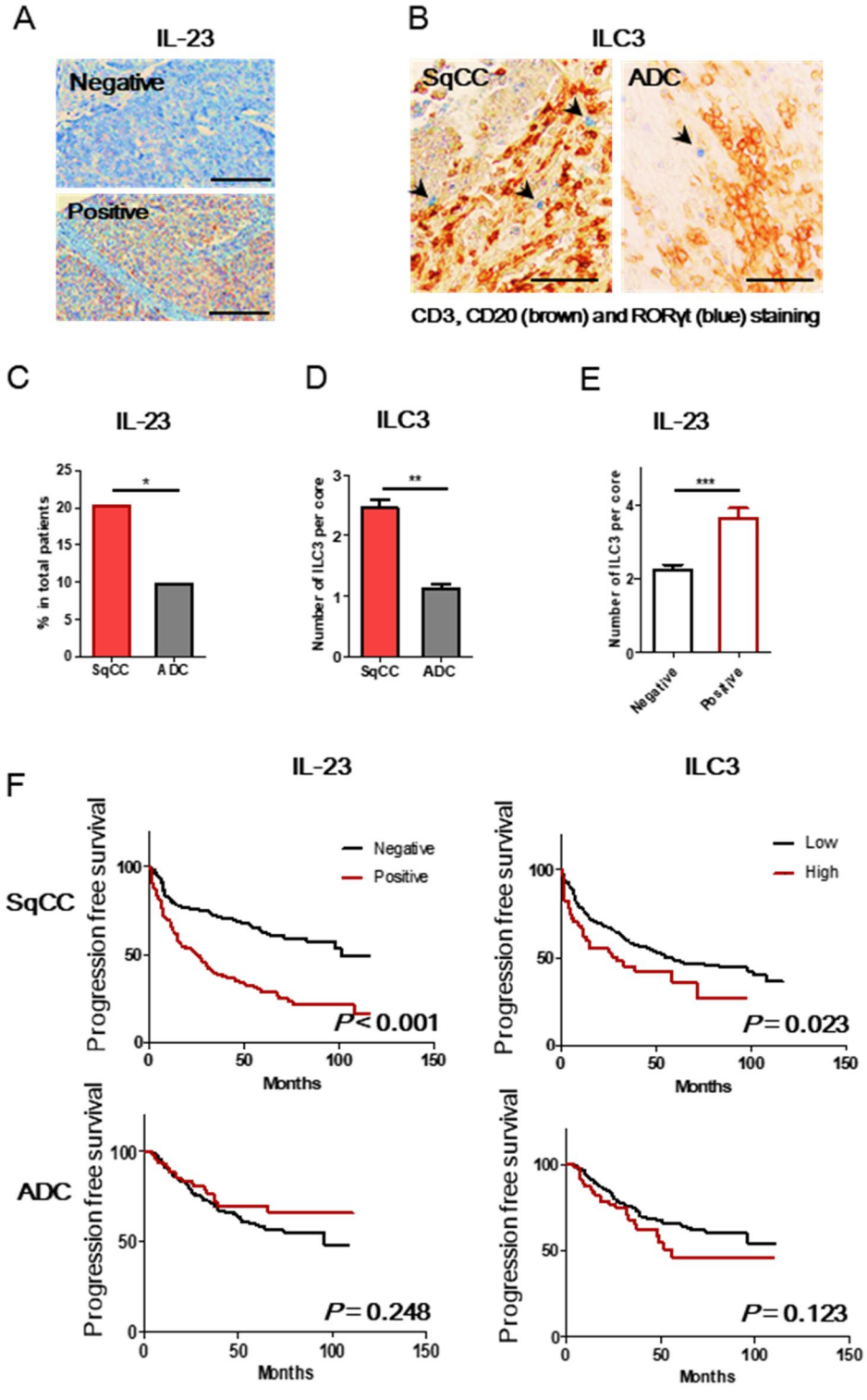
A
IL-23
Negative
Positive
B
ILC3
SqCC
ADC
CD3, CD20 (brown) and RORγt (blue) staining
C
IL-23
% in total patients
SqCC
ADC
D
ILC3
Number of ILC3 per core
SqCC
ADC
E
IL-23
Number of ILC3 per core
Negative
Positive
F
IL-23
ILC3
SqCC
ADC
Progression free survival
Months
Negative
Positive
Low
High
P< 0.001
P= 0.023
P= 0.248
P= 0.123

Figure 19. ILC3 contributes to the poor prognosis of patients with SqCC.

(**A**) Image of IL-23 expression in NSCLCs of retrospective cohort using immunohistochemistry. Scale bars, 200 μm. (**B**) Image of the expression of CD3 + CD20 (brown) and RORγt (blue) in SqCCs and ADCs of retrospective cohort using immunohistochemistry. Arrow indicates $CD3^-CD20^-ROR\gamma t^+$ ILC3 cells. Scale bars, 200 μm. (**C** and **D**) Percentages of $IL\text{-}23^+$ tumor cells and the numbers of $CD3^-CD20^-ROR\gamma t^+$ ILC3 cells in SqCCs and ADCs. (**E**) The numbers of $CD3^-CD20^-ROR\gamma t^+$ ILC3 cells were counted according to the expression of IL-23 in SqCCs and ADCs. (**F**) Progression-free survival of patients with SqCC or ADC was plotted using Kaplan-Meier analyses with the log-rank test according to the numbers of $CD3^-CD20^-ROR\gamma t^+$ ILC3 cells, which was estimated using immunohistochemistry. Data are presented as the mean ± SEM. *$p < 0.05$, **$p < 0.01$, ***$p < 0.001$.

4. Discussion

4.1 The conversion of ILC1 into ILC3 by tumor cells exists in TME

In this study, IL-17 expression ILC3 has increased in pulmonary SqCC and inverse correlation between ILC1 and ILC3 was found in pulmonary SqCCs. The conversion from ILC1 into ILC3 was promoted by IL-23-producing tumor cells, increased ILC3 promotes tumor cell proliferation by secreting IL-17. These findings indicate that cancer cells could modify a specific TME by the functional plasticity of ILCs, in particular, the conversion from ILC1 into ILC3. Regarding the mechanism of the conversion of ILCs, Bernink et al. reported that the combination treatment of IL-2, IL-23, and IL-1β promoted the conversion of $CD127^+$ ILC1 into IL-22-producing ILC3 in vitro, which was reversible and dependent on RORγt (57). They also demonstrated that $CD14^+$ DCs promoted polarization from ILC3 to ILC1, whereas $CD14^-$ DCs promoted the conversion from ILC1 into ILC3 (57). Moreover, the numbers of $CD127^+$ ILC1 increased at the expense of ILC3 in inflamed intestinal tissues from patients with Crohn's disease, whereas $CD127^+$ ILC1 converted into ILC3 in humanized mice in the absence of inflammation (57, 63). $CX3CR1^+$ DCs contribute to the homeostasis of $CXCR6^+$ $NKp46^-$ ILC3 by producing IL-23 and CXCL16 in the intestine (64). These findings suggest that the conversion between ILC1 and ILC3 and homeostasis of ILCs in the intestine may be regulated by hematopoietic cells rather than non-hematopoietic cells, depending on the

inflammatory status of the microenvironment. In contrast to the intestine, the percentages of $CD141^+$ DCs were not correlated with ILC subsets in my study. Furthermore, tumor cells from SqCCs, rather than ADCs, produced high levels of IL-23 and promoted the conversion of ILC1 into ILC3 in an IL-23-dependent manner. Thus, tumor cells, rather than hematopoietic cells, in the TME of SqCCs directly regulate the conversion from ILC1 into ILC3 by producing IL-23. However, SqCC tumor cells or recombinant IL-23 minimally affect conversion of SqCC-derived ILCs. Moreover, tumor cells of ADC failed to maintain high levels of ILC3 in SqCC-derived ILCs in co-culture, which was restored by adding recombinant IL-23. To explain these findings, it is hypothesized that conversion of ILC1 into ILC3 has been maximally achieved and maintained as plateau status in TME of SqCC. Combined, these findings suggest that IL-23 might exert effect on maintenance of ILC3 in addition to conversion of ILC1 into ILC3 in TME.

4.2 Novel finding of IL-23 mediated tumor survival strategy

In TME, tumor cells provide tumor cell proliferation signals and a suitable environment for tumor progression by modulating immune cells (65, 66). To this end, tumor cells employ diverse strategies, including decreasing the expression of antigen-presenting proteins, increasing the expression of inhibitory proteins in immune cells, and regulating the plasticity of Th cells and M1/M2 macrophages (15-18). In addition to these strategies, I suggest that the IL-23-producing tumor-mediated conversion from ILC1 into ILC3 is

a novel strategy of tumors that favors tumor progression and expansion in the TME. Similar to lung cancer, SqCCs in the esophagus also express IL-23, contributing to the epithelial-mesenchymal transition via the Wnt/β-catenin pathway (67). And keratinocyte can induce IL-23 expression by TLR signaling and so on. Regarding squamous epithelium is one component of keratinocyte, these findings suggest that IL-23 produced by SqCCs has diverse effects on tumorigenesis and progression by regulating intrinsic tumor biology and crosstalk with extrinsic immune cells, which suggests that the IL-23-ILC3 axis may be a therapeutic target for IL-23-producing SqCCs. Biological reagents that inhibit the IL-23 pathway have demonstrated efficacy in clinical trials for the treatment of inflammatory diseases including Crohn's disease and psoriasis (68, 69), which suggests that IL-23 blockade may be a useful therapeutic strategy for IL-23-mediated human diseases, including IL-23-producing lung cancers. However, no clinical trials have addressed human cancers using an IL-23 inhibitor or blockade. Moreover, the effects of IL-23 blockade on tumor progression may be diverse, because the biological effects of IL-23 on both tumor and immune cells are more complex, depending on the activation status of immune and tumor cells and the patient's clinical stages. Nevertheless, IL-23 blockade or an IL-23 inhibitor may efficiently suppress the progression of IL-23-producing lung cancers due to dual effects on the plasticity of both ILC3 and Th17 cells in the TME, although further study is needed to validate this strategy.

4.3 IL-23/ILC3/IL-17 axis: a critical pathway of tumor progression in SqCCs

Emerging studies have demonstrated that IL-17 promotes the progression and metastasis of lung cancer by increasing tumor angiogenesis, and cell proliferation but inhibiting apoptosis (70). However, whether IL-17 regulates tumor growth in specific histological types of NSCLCs, such as SqCCs and ADCs remains unknown. My experiments demonstrated that IL-17-IL-17R axis was enhanced in SqCCs relative to ADCs and contributed to a short survival of patients with SqCC, which suggests that IL-17-IL-17R axis contributes to tumor growth in SqCCs but not ADCs. Among the IL-17-expresssing immune cells, IL-17+ ILCs were higher in number in SqCCs than ADCs, whereas the expression level of IL-17 in CD3+ T cells from the two histological types was similar in transcriptome analyses. Moreover, co-culture experiments revealed that converted ILC3 promoted tumor growth in SqCCs by producing IL-17. These findings suggest that the tumor growth of SqCCs rather than ADCs may be attributable to higher numbers of IL-17-producing ILC3, although IL-17 produced by other immune cells similarly affects tumor growth of the two histological types of NSCLCs. Thus, it is feasible that increased numbers of ILC3 in SqCCs contribute more to tumor growth than ADCs. By contrast, it was suggested that NKp46-expressing ILC3 may inhibit tumor growth via the IL-12-dependent enhancement of adhesion molecules in blood vessels in melanoma (55). Moreover, Carrega et al. hypothesized that NCR^+ ILC3 has an anti-tumor effect on human lung cancer, because NCR^+ ILC3 upregulated the expression

of adhesion molecules in endothelial and mesenchymal stem cells in vitro and they were found in tertiary lymphoid structures (49). These contradictory outcomes between that study and my study may be due to the different cohorts of patients with different numbers of cases (50 cases in the study by Carrega et al. versus 80 cases in the current study) and/or histological types of NSCLC. However, it is unclear how many cases of SqCCs and ADCs were involved in previous study, although the authors reported no difference in the ILC population between the two histological types. Furthermore, they did not identify an inverse correlation between ILC1 and ILC3 in NSCLCs and did not directly address the functional role of ILC3 in tumor progression and the survival of patients with NSCLC. By contrast, my experiments clearly demonstrated that the numbers of CD3-RORγt+ ILC3 in the TME, and IL-17RA-expressing tumor cells were associated with a poor prognosis of patients with SqCCs but not ADCs. These findings suggest that the IL-23-ILC3-IL-17 axis is a critical pathway that promotes tumor growth of SqCCs, thereby shortening progression-free survival.

4.4 Conclusive remarks

In conclusion, these results demonstrate that IL-23-producing SqCCs promote IL-17-mediated tumor growth by converting ILC1 into ILC3 in the TME, thereby shortening patient survival. Furthermore, I believe that lung cancers may utilize the IL-23-ILC3-IL-17 axis to favor tumor growth and expansion in the TME, which suggests that this axis may be a useful therapeutic target of IL-23-producing lung cancers.

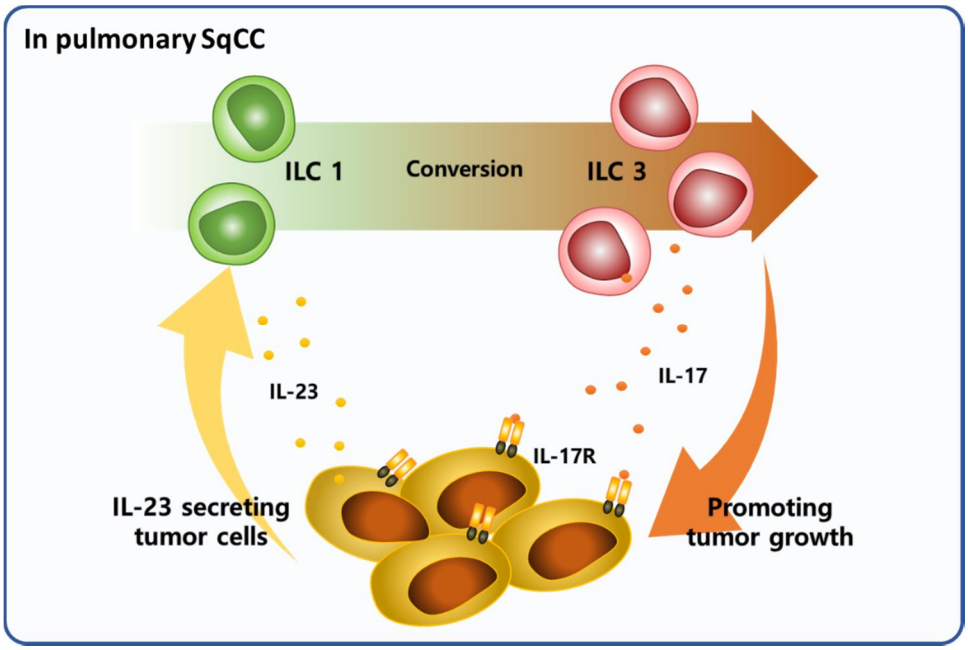

Figure 20. Graphical summary

TME of SqCC showed highly activated IL-17 axis than pulmonary ADC. So I analyzed IL-17 secreting immune subsets in TME, only ILC3 was distributed differently between SqCC and ADC. The number of ILC3 was negatively correlated with ILC1 in SqCC and positively correlated with IL-23 expression from tumor cells. According to *in vitro* and *in vivo* experiments demonstrate that IL-23 from tumor cells convert ILC1 into ILC3. And IL-17 from ILC3 affect poor prognosis of patients with pulmonary SqCC by mediating tumor cell proliferation.

Bibliography

1. Siegel RL, Miller KD, Jemal A. Cancer Statistics, 2017. CA: a cancer journal for clinicians. 2017;67:7-30.

2. Cancer Genome Atlas Research N. Comprehensive molecular profiling of lung adenocarcinoma. Nature. 2014;511:543-50.

3. Pan Y, Wang R, Ye T, Li C, Hu H, Yu Y, et al. Comprehensive analysis of oncogenic mutations in lung squamous cell carcinoma with minor glandular component. Chest. 2014;145:473-9.

4. Wozniak AJ, Gadgeel SM. Clinical presentation of non-small cell carcinoma of the lung. In: Pass HI, Carbone DP, Johnson DH, Minna JD, Scagliotti GV, Turrisi AT, eds. Principles and Practice of Lung Cancer. 4th ed. Philadelphia, Pa: Lippincott Williams & Wilkins. 2010:327-40.

5. Alberg AJ, Brock MV, Samet JM. Epidemiology of lung cancer: looking to the future. J Clin Oncol 2005;23(14):3175-85

6. Berthiller J, Straif K, Boniol M, Voirin N, Benhaim-Luzon V, Ayoub WB, et al. Cannabis smoking and risk of lung cancer in men: a pooled analysis of three studies in Maghreb. J Thorac Oncol 2008;3(12):1398-403

7. Detterbeck FC. Viewing Lung Cancer in Color Instead of Black and White. Ann Am Thorac Soc 2015;12(8):1118-9

8. Brahmer JR, Pardoll DM. Immune checkpoint inhibitors: making immunotherapy a reality for the treatment of lung cancer. Cancer immunology research. 2013;1:85-91.

9. Brahmer J, Reckamp KL, Baas P, Crino L, Eberhardt WE, Poddubskaya E, et al. Nivolumab versus Docetaxel in Advanced Squamous-Cell Non-Small-Cell Lung Cancer. N Engl J Med. 2015;373:123-35.

10. Borghaei H, Paz-Ares L, Horn L, Spigel DR, Steins M, Ready NE, et al. Nivolumab versus Docetaxel in Advanced Nonsquamous Non-Small-Cell Lung Cancer. N Engl J Med. 2015;373:1627-39.

11. Joyce JA, Pollard JW. Microenvironmental regulation of metastasis. Nat Rev Cancer 2009;9(4):239-52

12. Waugh DJ, Wilson C. The interleukin-8 pathway in cancer. Clin Cancer Res. (2008) 14:6735–41. 10.1158/1078-0432.ccr-07-4843

13. Vinay, D.S., Ryan, E.P., Pawelec, G., Talib, W.H., Stagg, J., Elkord, E., et al., 2015. Immune evasion in cancer: mechanistic basis and therapeutic strategies. Semin. Cancer Biol. 35 (Suppl), S185–S198

14. Gazdar AF. Activating and resistance mutations of EGFR in non-small-cell lung cancer: role in clinical response to EGFR tyrosine kinase inhibitors. Oncogene. 2009;28:S24–S31.

15. So T., Takenoyama M., Mizukami M., Ichiki Y., Sugaya M., Hanagiri T., et al. (2005). Haplotype loss of HLA class I antigen as an escape mechanism from immune attack in lung cancer. *Cancer Res.*65 5945–5952. 10.1158/0008-5472.Can-04-3787

16. Juneja V. R., McGuire K. A., Manguso R. T., et al. PD-L1 on tumor cells is sufficient for immune evasion in immunogenic tumors and inhibits CD8 T cell cytotoxicity. J Exp Med. 2017;214(4):895–904. doi: 10.1084/jem.20160801.

17. Leveque L, Deknuydt F, Bioley G, Old LJ, Matsuzaki J, Odunsi K, Ayyoub M, Valmori D. Interleukin 2-mediated conversion of ovarian cancer-associated $CD4^+$ regulatory T cells into proinflammatory interleukin 17-producing helper T cells. J Immunother. 2009;32:101–108.

18. Mantovani A, Sozzani S, Locati M, Allavena P, Sica A. Macrophage polarization: tumor-associated macrophages as a paradigm for polarized M2 mononuclear phagocytes. Trends Immunol. 2002;23:549–555.

19. Rouvier E, Luciani MF, Mattei MG, Denizot F, Golstein P. CTLA-8, cloned from an activated T cell, bearing AU-rich messenger RNA instability sequences, and homologous to a herpesvirus saimiri gene. J Immunol 1993;150(12):5445-56.

20. Yao Z, Fanslow WC, Seldin MF, Rousseau AM, Painter SL, Comeau MR, et al. Herpesvirus Saimiri encodes a new cytokine, IL-17, which binds to a novel cytokine receptor. Immunity 1995;3(6):811-21.

21. Hymowitz SG, Filvaroff EH, Yin JP, Lee J, Cai L, Risser P, et al. IL-17s adopt a cystine knot fold: structure and activity of a novel cytokine,

IL-17F, and implications for receptor binding. EMBO J 2001;20(19):5332-41

22. Moseley TA, Haudenschild DR, Rose L, Reddi AH. Interleukin-17 family and IL-17 receptors. Cytokine Growth Factor Rev 2003;14(2):155-74.

23. Gaffen SL. Biology of recently discovered cytokines: interleukin-17--a unique inflammatory cytokine with roles in bone biology and arthritis. Arthritis Res Ther 2004;6(6):240-7

24. Nam JS, Terabe M, Kang MJ, Chae H, Voong N, Yang YA, et al. Transforming growth factor beta subverts the immune system into directly promoting tumor growth through interleukin-17. Cancer Res 2008;68(10):3915-23

25. Veldhoen M. Interleukin 17 is a chief orchestrator of immunity. Nat Immunol. 2017;18:612-21.

26. Qian X, Chen H, Wu X, Hu L, Huang Q, Jin Y. Interleukin-17 acts as double-edged sword in anti-tumor immunity and tumorigenesis. Cytokine. 2017;89:34-44.

27. Shime H, Yabu M, Akazawa T, Kodama K, Matsumoto M, Seya T, et al. Tumor-secreted lactic acid promotes IL-23/IL-17 proinflammatory pathway. J Immunol 2008;180(11):7175-83

28. Murugaiyan G, Mittal A, Weiner HL. Increased osteopontin expression in dendritic cells amplifies IL-17 production by CD4+ T cells in experimental autoimmune encephalomyelitis and in multiple sclerosis. J Immunol 2008;181(11):7480-8

29. Chizzolini C, Chicheportiche R, Alvarez M, de Rham C, Roux-Lombard P, Ferrari-Lacraz S, et al. Prostaglandin E2 synergistically with interleukin-23 favors human Th17 expansion. Blood 2008;112(9):3696-703

30. Spits H, Artis D, Colonna M, Diefenbach A, Di Santo JP, Eberl G, et al. Innate lymphoid cells--a proposal for uniform nomenclature. Nat Rev Immunol. 2013;13:145-9.

31. Spits H, Cupedo T. Innate lymphoid cells: emerging insights in development, lineage relationships, and function. Annu Rev Immunol 2012;30:647-75

32. Yokota Y, Mansouri A, Mori S, Sugawara S, Adachi S, Nishikawa S, et al. Development of peripheral lymphoid organs and natural killer cells depends on the helix-loop-helix inhibitor Id2. Nature 1999;397(6721):702-6

33. Spits H, Di Santo JP. The expanding family of innate lymphoid cells: regulators and effectors of immunity and tissue remodeling. Nat Immunol 2011;12(1):21-7

34. Buonocore S, Ahern PP, Uhlig HH, Ivanov, II, Littman DR, Maloy KJ, et al. Innate lymphoid cells drive interleukin-23-dependent innate intestinal pathology. Nature. 2010;464:1371-5.

35. Kim HY, Umetsu DT, Dekruyff RH. Innate lymphoid cells in asthma: Will they take your breath away? Eur J Immunol. 2016;46:795-806.

36. O'Sullivan TE, Rapp M, Fan X, Weizman OE, Bhardwaj P, Adams NM, et al. Adipose-Resident Group 1 Innate Lymphoid Cells Promote Obesity-Associated Insulin Resistance. Immunity. 2016;45:428-41.

37. van Beek JJP, Martens AWJ, Bakdash G, de Vries IJM. Innate Lymphoid Cells in Tumor Immunity. Biomedicines. 2016;4.

38. Biron CA. Natural killer cell regulation during viral infection. Biochem Soc Trans 1997;25(2):687-90.

39. Biron CA. Activation and function of natural killer cell responses during viral infections. Curr Opin Immunol 1997;9(1):24-34.

40. Mattner J, Wirtz S. Friend or Foe? The Ambiguous Role of Innate Lymphoid Cells in Cancer Development. Trends Immunol. 2017;38:29-38.

41. Walker JA, Barlow JL, McKenzie AN. Innate lymphoid cells--how did we miss them? Nat Rev Immunol 2013;13(2):75-87

42. Zaiss DM, Yang L, Shah PR, Kobie JJ, Urban JF, Mosmann TR. Amphiregulin, a TH2 cytokine enhancing resistance to nematodes. Science 2006;314(5806):1746

43. Sonnenberg GF, Fouser LA, Artis D. Border patrol: regulation of immunity, inflammation and tissue homeostasis at barrier surfaces by IL-22. Nat Immunol 2011;12(5):383-90

44. Grivennikov SI, Greten FR, Karin M. Immunity, inflammation, and cancer. Cell 2010;140(6):883-99

45. Nowarski R, Gagliani N, Huber S, Flavell RA. Innate immune cells in inflammation and cancer. Cancer Immunol Res 2013;1(2):77-84

46. Vallentin B, Barlogis V, Piperoglou C, Cypowyj S, Zucchini N, Chene M, et al. Innate Lymphoid Cells in Cancer. Cancer Immunol Res 2015;3(10):1109-14

47. Rub A, Dey R, Jadhav M, Kamat R, Chakkaramakkil S, Majumdar S, et al. Cholesterol depletion associated with Leishmania major infection alters macrophage CD40 signalosome composition and effector function. Nat Immunol 2009;10(3):273-80

48. Jovanovic IP, Pejnovic NN, Radosavljevic GD, Pantic JM, Milovanovic MZ, Arsenijevic NN, et al. Interleukin-33/ST2 axis promotes breast cancer growth and metastases by facilitating intratumoral accumulation of immunosuppressive and innate lymphoid cells. Int J Cancer 2014;134(7):1669-82

49. Carrega P, Loiacono F, Di Carlo E, Scaramuccia A, Mora M, Conte R, et al. NCR(+)ILC3 concentrate in human lung cancer and associate with intratumoral lymphoid structures. Nature communications. 2015;6:8280.

50. Numasaki M, Fukushi J, Ono M, Narula SK, Zavodny PJ, Kudo T, et al. Interleukin-17 promotes angiogenesis and tumor growth. Blood 2003;101(7):2620-7

51. Chen X, Xie Q, Cheng X, Diao X, Cheng Y, Liu J, et al. Role of interleukin-17 in lymphangiogenesis in non-small-cell lung cancer: Enhanced production of vascular endothelial growth factor C in non-small-cell lung carcinoma cells. Cancer Sci 2010;101(11):2384-90

52. Ikutani M, Yanagibashi T, Ogasawara M, Tsuneyama K, Yamamoto S, Hattori Y, et al. Identification of innate IL-5-producing cells and their role in lung eosinophil regulation and antitumor immunity. J Immunol. 2012;188:703-13.

53. Kirchberger S, Royston DJ, Boulard O, Thornton E, Franchini F, Szabady RL, et al. Innate lymphoid cells sustain colon cancer through production of interleukin-22 in a mouse model. J Exp Med. 2013;210:917-31.

54. Cella M, Otero K, Colonna M. Expansion of human NK-22 cells with IL-7, IL-2, and IL-1beta reveals intrinsic functional plasticity. Proc Natl Acad Sci U S A 2010;107(24):10961-6

55. Eisenring M, vom Berg J, Kristiansen G, Saller E, Becher B. IL-12 initiates tumor rejection via lymphoid tissue-inducer cells bearing the natural cytotoxicity receptor NKp46. Nat Immunol. 2010;11:1030-8.

56. Fang D, Zhu J. Dynamic balance between master transcription factors determines the fates and functions of CD4 T cell and innate lymphoid cell subsets. J Exp Med. 2017;214:1861-76.

57. Bernink JH, Krabbendam L, Germar K, de Jong E, Gronke K, Kofoed-Nielsen M, et al. Interleukin-12 and -23 Control Plasticity of CD127(+) Group 1 and Group 3 Innate Lymphoid Cells in the Intestinal Lamina Propria. Immunity. 2015;43:146-60.

58. Vonarbourg C, Mortha A, Bui VL, Hernandez PP, Kiss EA, Hoyler T, et al. Regulated expression of nuclear receptor RORgammat confers distinct functional fates to NK cell receptor-expressing RORgammat(+) innate lymphocytes. Immunity 2010;33(5):736-51

59. Ren S, Peng Z, Mao JH, Yu Y, Yin C, Gao X, et al. RNA-seq analysis of prostate cancer in the Chinese population identifies recurrent gene fusions, cancer-associated long noncoding RNAs and aberrant alternative splicings. Cell Res. 2012;22:806-21.

60. Yang B, Kang H, Fung A, Zhao H, Wang T, Ma D. The role of interleukin 17 in tumour proliferation, angiogenesis, and metastasis. Mediators of inflammation. 2014;2014:623759.

61. Webster KE, Kim HO, Kyparissoudis K, Corpuz TM, Pinget GV, Uldrich AP, et al. IL-17-producing NKT cells depend exclusively on IL-7 for homeostasis and survival. Mucosal immunology. 2014;7:1058-67.

62. Nembrini C, Marsland BJ, Kopf M. IL-17-producing T cells in lung immunity and inflammation. J Allergy Clin Immunol. 2009;123:986-94; quiz 95-6.

63. Bernink JH, Peters CP, Munneke M, te Velde AA, Meijer SL, Weijer K, et al. Human type 1 innate lymphoid cells accumulate in inflamed mucosal tissues. Nat Immunol. 2013;14:221-9.

64. Satoh-Takayama N, Serafini N, Verrier T, Rekiki A, Renauld JC, Frankel G, et al. The chemokine receptor CXCR6 controls the functional topography of interleukin-22 producing intestinal innate lymphoid cells. Immunity. 2014;41:776-88.

65. Kuan EL, Ziegler SF. A tumor-myeloid cell axis, mediated via the cytokines IL-1alpha and TSLP, promotes the progression of breast cancer. Nat Immunol. 2018;19:366-74.

66. Terra M, Oberkampf M, Fayolle C, Rosenbaum P, Guillerey C, Dadaglio G, et al. Tumor-derived TGF-beta alters the ability of plasmacytoid dendritic cells to respond to innate immune signaling. Cancer research. 2018.

67. Chen D, Li W, Liu S, Su Y, Han G, Xu C, et al. Interleukin-23 promotes the epithelial-mesenchymal transition of oesophageal carcinoma cells via the Wnt/beta-catenin pathway. Scientific reports. 2015;5:8604.

68. Feagan BG, Sandborn WJ, D'Haens G, Panes J, Kaser A, Ferrante M, et al. Induction therapy with the selective interleukin-23 inhibitor risankizumab in patients with moderate-to-severe Crohn's disease: a randomised, double-blind, placebo-controlled phase 2 study. Lancet. 2017;389:1699-709.

69. Dong J, Goldenberg G. New biologics in psoriasis: an update on IL-23 and IL-17 inhibitors. Cutis. 2017;99:123-7.

70. Wu F, Xu J, Huang Q, Han J, Duan L, Fan J, et al. The Role of Interleukin-17 in Lung Cancer. Mediators of inflammation. 2016;2016:8494079.

국문초록

폐암 세포 유래 인터루킨-23에 의한 선천성 림프구 세포 1형에서 3형으로의 변환이 종양 성장에 미치는 영향 연구

최근 PD-1 을 비롯한 면역 치료가 환자에게 좋은 반응을 보이면서 종양 미세환경에 존재하는 면역세포에 대한 이해가 그 어느 때보다 중요해지고 있다. 선천성 림프구 세포는 선천성 면역세포에 가깝지만 도움 T 세포에 상응하는 역할을 담당하는 특징을 가진 비교적 최근에 밝혀진 세포군이다. 선천성 림프구 세포는 각 발현하는 전사인자 및 분비하는 사이토카인을 통해 3 가지 아형으로 나뉜다. 선천성 림프구 세포 아형 간 형질 전환은 대장염 실험 모델에서 보고된 바 있으나 종양에서는 아직까지 밝혀진 내용이 없고, 선천성 림프구 세포의 아형별 종양 미세환경에서의 역할에 대하여 아직까지 정립되지 않았다. 또한, 선천성 림프구 세포 3 형을 비롯한 여러 종류의 면역 세포가 분비할 수 있는 물질 중 하나인 인터루킨-17 이 종양에 미치는 영향에 대해서는 연구마다 다른 결과를 제시하고 있어 아직까지 더 많은 연구가 필요하다. 이번 연구는 선천성 림프구 세포가 폐암 조직 내에 존재 및 형질 전환

발생 여부, 종양 내에서의 역할을 파악해 봄으로써 새로운 면역 치료 타겟을 발굴하고자 계획하게 되었다.

2015 년부터 2017 년까지 서울대학교병원에서 비소세포폐암으로 절제술을 받은 환자 80 명의 신선 상태의 종양과 정상 폐 조직을 대상으로 각 조직 내 존재하는 면역 세포의 분포 및 발현 물질을 파악하였다. 또한 신선 종양 조직에서 선천성 림프구 세포를 얻은 뒤 비소세포 폐암 세포주 혹은 환자 조직으로부터 얻은 종양 세포와 함께 배양하여 나타나는 변화를 파악하였고, 마우스 종양 모델을 구축하여 생체 내에서의 종양 성장 변화를 확인하였다. 또한 2001 년부터 2012 년까지 동일 기관에서 비소세포폐암으로 폐엽 절제술을 시행한 환자들의 파라핀 블록에서 종양 부위만을 획득하여 조직 미세배열 블록을 제작 및 면역조직화학 염색을 시행하여 임상 지표와의 연관성 및 생존 분석을 시행하였다.

우선 종양 세포에서의 인터루킨-17 수용체 발현과 주변 면역 세포들의 인터루킨-17 의 발현을 조사하였을 때 선암에 비해 편평상피세포암에서 두 인자 모두 높게 발현하고 있음을 확인하였다. 인터루킨-17 을 분비할 수 있는 여러 면역 세포군 중에서는 유일하게 선천성 림프구 세포 3 형이 폐 편평상피세포암에서 선암이나 정상 폐 조직에 비해 많이 존재함을 관찰하였고 선천성 림프수 세포 아형의 분포를 파악하였을 때 편평상피세포암에서 3 형이 1 형보다 종양 내에 많이 분포하고 있었으나 선암에서는 정상 조직과 큰 차이를 보이지 않았다.

이러한 분포의 차이는 아형별 전환을 유도할 수 있는 사이토카인 분비에 의할 것이라는 가정 하에 사이토카인 분비와 선천성 림프구 세포 1 형, 3 형과의 연관성을 확인하였다. 그 중 종양 세포에서 발현되는 인터루킨-23 이 선천성 림프구 1 형과 역상관관계를, 3 형과 정상관관계를 보였다. 공생배양 실험을 하였을 때 편평상피세포암 세포와 선천성 림프구 전체 혹은 1 형을 함께 배양한 경우에 3 형 의 증가를 보였고, 종양 세포의 증식 증가를 확인하였다. 추가적으로 마우스 및 마우스 편평상피세포암 세포주를 이용하여 실험을 하였을 때에도 인터루킨-23 과발현 종양 세포를 투여한 마우스에서 종양 세포의 증식 증가 및 선천성 림프구 세포 1 형 이 3 형으로 전환되는 현상과 인터루킨-17 의 증가를 확인하여 생체 내에서도 같은 현상을 보임을 증명하였다.

마지막으로 종양 조직에서 면역조직화학염색을 통해 종양 세포에서 분비되는 인터루킨-23 의 발현 증가와 선천성 림프구 세포 3 형 의 증가가 편평상피암에서 관찰됨을 확인하였다. 또한 편평상피암 환자에서만 생존 분석에서 두 인자 모두 불량한 예후와 연관됨을 확인함으로써 종양이 자가 생존 및 성장을 위해 주변 면역세포, 그 중에서도 선천성 림프구 세포의 형질 전환을 유도할 수 있는 물질을 분비하여 자가 증식에 이용함을 최초로 보고하였다.

결론적으로 본 연구자는 편평상피세포폐암에서 발현하는 인터루킨-23 이 종양 내 미세환경에 존재하는 선천성 림프구 세포 1 형을 3 형으로 전환시켜 종양 내 인터루킨-17 축적의 증가를

유도하고, 이로 인해 인터루킨-17 기전에 의한 종양 성장 촉진이 환자의 불량한 예후로 이어지게 된다는 사실을 밝혔다.

본 연구는 선천성 림프구 세포를 이용한 종양의 생존 전략을 규명함으로써 폐암, 그 중에서도 편평상피세포암과 같이 인터루킨-23 을 많이 분비하는 종양에 대해 인터루킨-23/ 선천성 림프구 세포 3/ 인터루킨-17 축의 한 부분을 차단함으로써 환자의 생존률 향상이 가능한 치료 타겟을 제시하는 근거로 사용될 수 있을 것으로 기대된다.

……...

주요어: 선천성 림프구 세포, 가소성, 인터루킨-23, 인터루킨-17, 종양 미세환경, 비소세포 폐암

학번: 2012-21730